NUMERICAL EXPERIMENTS WITH A FIVE-LEVEL GLOBAL ATMOSPHERIC PREDICTION MODEL USING A STAGGERED, SPHERICAL, SIGMA COORDINATE SYSTEM

William Theodore Elias

NAVAL POSTGRADUATE SCHOOL
Monterey, California

THESIS

NUMERICAL EXPERIMENTS WITH A FIVE-LEVEL GLOBAL ATMOSPHERIC PREDICTION MODEL USING A STAGGERED, SPHERICAL, SIGMA COORDINATE SYSTEM

by

William Theodore Elias

Thesis Advisors: George Haltiner
Roger Williams

March 1973

Numerical Experiments with a Five-Level Global Atmospheric Prediction Model Using a Staggered, Spherical, Sigma Coordinate System

by

William Theodore Elias
Lieutenant, United States Navy
B.S., California Polytechnic College at Pomona, 1968

Submitted in partial fulfillment of the
requirements for the degree of

MASTER OF SCIENCE IN METEOROLOGY

from the

NAVAL POSTGRADUATE SCHOOL

March 1973

ABSTRACT

Three cases of analytic data and one case of real data were numerically integrated using a 5-level baroclinic primitive equations model of the general circulation. Experiments were performed using initial winds derived from the linear balance equation and also winds derived analytically. The feasibility of using the linear balance equation to initialize the wind field was examined. In all cases, the forecasts remained meteorological and reasonably well-behaved. Nevertheless, the forecasts derived from initial winds generated by the linear balance equation excited large, operationally-undesirable inertial-gravity waves, while the forecasts from analytically determined initial winds remained virtually free of such small scale "noise".

TABLE OF CONTENTS

I. INTRODUCTION ---------- 11

II. BAROCLINIC PRIMITIVE EQUATION MODEL ---------- 12

A. PRIMITIVE EQUATIONS ---------- 12

B. GRID ---------- 14

C. VERTICAL LAYERING ---------- 14

D. TIME DIFFERENCING ---------- 17

III. INITIAL CONDITIONS ---------- 19

A. ANALYTIC WINDS ---------- 22

B. DERIVED WINDS ---------- 23

IV. FOURIER WAVE ANALYSIS METHOD ---------- 25

V. RESULTS ---------- 26

VI. CONCLUSIONS ---------- 56

LIST OF REFERENCES ---------- 58

INITIAL DISTRIBUTION LIST ---------- 60

FORM DD 1473 ---------- 64

LIST OF CHARTS

A. Initial Surface Pressure Analysis (Experiment IV) ---------- 40

B. Verifying Surface Pressure Analysis (Experiment IV) ---------- 41

C. 12-Hour Forecast Using FNWC Model (Experiment IV) ---------- 42

D. 12-Hour Forecast Using Global Model (Experiment IV) ---------- 43

E. Initial Surface Pressure Analysis (Experiment I) ---------- 44

F. 12-Hour Surface Pressure Forecast Using Analytic and Derived Winds (Experiment I) ---------- 45

G. 24-Hour Surface Pressure Forecast Using Analytic and Derived Winds (Experiment I) ---------- 46

H. 36-Hour Surface Pressure Forecast Using Analytic and Derived Winds (Experiment I) ---------- 47

I. Initial Surface Pressure Analysis (Experiment II) ---------- 48

J. 12-Hour Surface Pressure Forecast Using Analytic and Derived Winds (Experiment II) ---------- 49

K. 24-Hour Surface Pressure Forecast Using Analytic and Derived Winds (Experiment II) ---------- 50

L. 36-Hour Surface Pressure Forecast Using Analytic and Derived Winds (Experiment II) ---------- 51

M. Initial Surface Pressure Analysis (Experiment III) ---------- 52

N. 6-Hour and 12-Hour Surface Pressure Forecast Using Analytic Winds (Experiment III) ---------- 53

O. 18-Hour and 24-Hour Surface Pressure Forecast Using Analytic Winds (Experiment III) ---------- 54

P. 30-Hour and 36-Hour Surface Pressure Forecast Using Analytic Winds (Experiment III) ---------- 55

LIST OF FIGURES

1. Location of Variables ---------- 15

2. Vertical Layering ---------- 16

3. Plot of Terrain Pressure Versus Forecast Hour at 0°N 15°E (Experiment IV) ---------- 34

4. Plot of Terrain Pressure Versus Forecast Hour at 40°N 15° E (Experiment IV) ---------- 35

5. Plot of Terrain Pressure Versus Forecast Hour at 85°N 15°E (Experiment IV) ---------- 36

6. Plot of Terrain Pressure Versus Forecast Hour at 0°N 15°E for "Analytic" Winds (Experiment II) ---------- 37

7. Plot of Terrain Pressure Versus Forecast Hour at 40°N 15°E for "Analytic" Winds (Experiment II) ---------- 38

8. Plot of Terrain Pressure Versus Forecast Hour at 85°N 15°E for "Analytic" Winds (Experiment II) ---------- 39

LIST OF TABLES

I. Wave Amplitudes and Mean Heights For Selected Latitutdes and Forecast Time ---------- 31

II. Computed Phase Speeds at Selected Latitudes Along with Method of Balancing and the Time Required To Make A 36-Hour Forecast For Each Experiment ---------- 32

III. Comparison of 12-Hour Forecast Pressures of the FNWC Model and the Global Model Against the Verifying Pressure Analysis ---------- 33

LIST OF SYMBOLS AND ABBREVIATIONS

A - Arbitrary constant in the stream function

A_m - Arbitrary constant for the Fourier series cosine terms

a - Earth's radius

B - Arbitrary constant in the stream function

B_m - Arbitrary constants for the Fourier series sine terms

CDC - Control Data Corporation

C_m - Arbitrary constants for the Fourier series combined terms

c_P - Specific heat for dry air at constant pressure

c - Wave speed

D - Lateral diffusion for the quantity indicated by the subscript

D_T - Lateral diffusion of heat

D_q - Lateral diffusion of specific humidity

D_m - Lateral diffusion of momentum

FNWC - Fleet Numerical Weather Central

F - Frictional stress

f - Coriolis parameter

$\bar{f}$ - Coriolis parameter at 45° north

g - Acceleration of gravity

H - Diabatic heating

i - Grid index in the x-direction (east-west)

j - Grid index in the y-direction (north-south)

M - Stands for ϕ, T, q, and w

m - Wave number

mb - Millibars

NPS - Naval Postgraduate School

NACA - National Advisory Committee on Aeronautics

N - Wave number plus one - m + 1

n - Degree of the Legrendre function

P - Pressure

P_n^m - Legrendre function of order m and degree n

Q - Moisture source/sink term

q - Specific humidity

R - Specific gas constant for dry air

t - Time

u - Zonal Wind

$\vec{V}$ - Horizontal vector velocity - (u,v)

v - Meridional wind

W - Stands for u and v

w - Measure of vertical velocity, positive upward
$w = -\dot{\sigma} = -\frac{d\sigma}{dt}$

Δt - Time increment

Δx - Distance increment in the x-direction - a $\Delta\lambda \cos\theta$

α - Specific volume

δ_m - Phase angle for wave number m

θ - Latitude, positive northward from south pole

$\Delta\theta$ - Distance increment in the latitudinal direction

λ - Longitude, positive eastward from Greenwich

$\Delta\lambda$ - Distance increment in longitudinal direction

ν - Angular wave velocity

π - Terrain pressure parameter

σ - Dimensionless vertical coordinate, $0 \leq \sigma \leq 1$, increasing downward

$\dot{\sigma}$ - Measure of vertical velocity - $\frac{d\sigma}{dt}$, -w

ϕ - Geopotential

ψ - Stream function

∇ - Del operator (horizontal)

∇^2 - Laplacian operator (horizontal)

ACKNOWLEDGEMENTS

The author wishes to express his thanks to Dr. G. J. Haltiner for his encouragement to undertake this project, Dr. R. T. Williams for his patient guidance without which this project would never have been completed, and Dr. F. J. Winninghoff for providing the original program.

In addition, the computer support of FNWC, under the command of Captain W. S. Houston Jr. USN, was both essential and greatly appreciated. The author would also like to express his thanks to several members of Captain Houston's staff, particularly Commander Celia L. Barteau, USN, and Mr. Leo Clarke who provided coordination of computer services.

I. INTRODUCTION

In the field of operational numerical weather prediction, the tendency, in recent years, has been toward the development of sophisticated global prediction models. This has been made possible by the rapid growth of computing capacity and developments connected with general circulation research.

The purpose of this study was to examine a baroclinic primitive equation model using a global, staggered, spherical, sigma coordinate system which could be used on an operational day to day basis by the United States Navy. In order to do this, an input procedure was developed to allow a real time initialization from FNWC analysis fields. A set of analytic fields using an analytic spherical harmonic stream function, first presented by Neamtan (1946), was also developed for use as a controlled set of initial conditions. By using these analytic cases, errors in real data collection, analysis and initialization, which are inevitable in practical meteorology, were avoided. The use of an analytic case also allowed the control of temperature and moisture distribution, predominant wave number, phase speed and wave amplitude.

The objective was to isolate and correct problems in the model by using the controlled analytic input with the ultimate aim of improving and extending the Navy's overall capability to predict weather phenomena on a global scale.

II. BAROCLINIC PRIMITIVE EQUATION MODEL

The governing differential equations, written in vector form, are similar to sets used by Smagorinsky et al. (1965), Arakawa et al. (1969) and Kesel and Winninghoff (1972). The integrations were carried out on a global, spherical, staggered, sigma coordinate system using the conservative-type difference equations based on the work of Arakawa (1966). The complete set of finite difference equations are given in Kesel and Winninghoff (1972) for the non-staggered square grid. The Arakawa type spatial differencing was used to eliminate the spurious energy growth which can occur with the more conventional finite difference approximations to the nonlinear advection terms.

A. PRIMITIVE EQUATIONS

The vector equation of horizontal motion in the sigma (σ) coordinate system for this model is:

$$\frac{\partial}{\partial t}(\pi\vec{V}) + (\nabla\cdot\pi\vec{V})\vec{V} + \pi\frac{\partial}{\partial\sigma}(\dot{\sigma}\vec{V}) + f(\vec{K}X\pi\vec{V}) + \pi\nabla\phi + \sigma\pi\alpha\nabla\pi = \vec{F} + \vec{D}_m$$

The Thermodynamic energy equation is:

$$\frac{\partial}{\partial t}(\pi T) + \nabla\cdot(\pi T\vec{V}) + \pi\frac{\partial}{\partial\sigma}(T\dot{\sigma}) - \frac{\pi\alpha}{c_p}(\sigma\frac{\partial\pi}{\partial t} + \sigma\vec{V}\cdot\nabla\pi + \pi\dot{\sigma}) = \pi H + D_T$$

The mass continuity equation is:

$$\frac{\partial \pi}{\partial t} + \nabla \cdot (\pi \vec{V}) + \pi \frac{\partial \dot{\sigma}}{\partial \sigma} = 0$$

The moisture continuity equation is:

$$\frac{\partial}{\partial t}(\pi q) + \nabla \cdot (\pi q \vec{V}) + \pi \frac{\partial}{\partial \sigma}(q\dot{\sigma}) = \pi Q + D_q$$

These equations are supplemented by the hydrostatic equation

$$\frac{\partial \phi}{\partial \sigma} + \pi \alpha = 0$$

the equation of state

$$\alpha = RT/P$$

and the dimensionless vertical coordinate

$$\sigma = P/\pi$$

In the above equations, u is the zonal wind component; v, the meridional wind component; π, the terrain pressure; $\dot{\sigma}$ the vertical-velocity measure; T, the temperature; f, the Coriolis parameter; ϕ, the geopotential; q, the specific humidity; H, the diabatic heating; $\vec{F}$, the frictional stress;

$\vec{D}_m$, the lateral diffusion of momentum; D_T, the lateral diffusion of heat; D_q, the lateral diffusion of moisture; Q, the moisture source/sink term and P, the pressure. Furthermore, the formulations for frictional stress ($\vec{F}$), lateral diffusion (D), heating (H) and moisture (Q) are identical to those described in Kesel and Winninghoff (1972).

B. GRID

The spatial finite differencing was performed on a staggered, spherical grid. The geopotential (ϕ), temperature (T), specific humidity (q) and the vertical-velocity measure ($w = -\dot{\sigma}$) were carried at the poles. The longitudinal and latitudinal grid increments were both five degrees. This gives 2520 points over the globe, with (ϕ,T,q,w) and (u,v) carried at 1260 points each (See Fig. 1). When ϕ,T,q or w variables are needed at (u,v) points (e.g. T in the friction term and w in the vertical advection of momentum term), they are defined as the average of the 4 values at the surrounding (ϕ,T,q,w) points.

C. VERTICAL LAYERING

The present model divides the atmosphere into five layers, as sketched in Figure 2. The basic variables of the model are carried at the center of each layer. Additional variables and conditions are specified at the interface between layers, as well as the upper and lower boundaries.

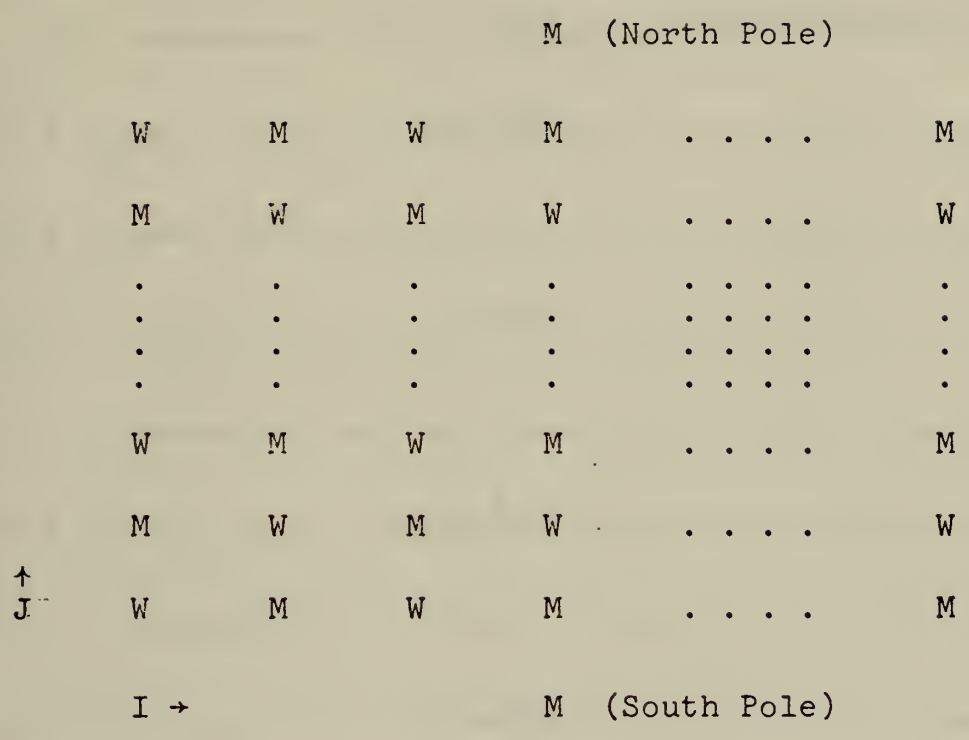

FIGURE 1. LOCATION OF VARIABLES

M stands for ϕ, T, q and w variables
W stands for u and v variables

Pressure	Computed Variables (at each level)	Level (Notational Subscript)	Sigma (σ)
0.0	w = 0	UPPER BOUNDARY	0.0
.1 × π	u,v,T,ϕ	5	0.1
.2 × π	w	4	0.2
.3 × π	u,v,T,ϕ	4	0.3
.4 × π	w	3	0.4
.5 × π	u,v,T,ϕ,q	3	0.5
.6 × π	w	2	0.6
.7 × π	u,v,T,ϕ,q	2	0.7
.8 × π	w	1	0.8
.9 × π	u,v,T,ϕ,q	1	0.9
π	w = 0	LOWER BOUNDARY	1.0

FIGURE 2. VERTICAL LAYERING

In the above figure, sigma (σ) is the dimensionless vertical coordinate, u, is the zonal wind component, v is the meridional wind component, q is the specific humidity, ϕ is the geopotential, π is the terrain pressure and w is the vertical-velocity measure ($-\dot{\sigma}$).

Integrations are performed in the Phillip's (1957) sigma (σ) coordinate system, where pressure, P, is normalized with the underlying terrain pressure, π. The dimensionless vertical coordinate, sigma (σ), is defined as

$$\sigma = P/\pi$$

It follows that

$\sigma = 1$ at the earth's surface

and $\sigma = 0$ at the top of the atmosphere.

The zonal wind component (u), the meridional wind component (v), the temperature (T) and geopotential (ϕ) are carried at sigma levels .9, .7, .5, .3 and .1. The specific humidity (q) is carried at sigma levels .9, .7 and .5. The vertical velocity measure, $w = -\dot{\sigma}$, is calculated diagnostically from the continuity equation for the layer interfaces. The vertical-velocity measure (w) is carried at sigma lev ls .8, .6, .4 and .2.

D. TIME DIFFERENCING

The two finite difference techniques that were used to step forward in time are the centered (leapfrog) difference scheme and the Matsuno (Euler backward) difference scheme. The finite difference equation for the centered technique is:

$$F^{t+1} = F^{t-1} + 2\Delta t \frac{\partial F^t}{\partial t}$$

Since the form has three time levels, it has both a physical and a computational mode (Haltiner, 1971). This computational mode, which changes phase at every time step, causes the solutions at adjacent time steps to become decoupled. Furthermore, the centered scheme is not feasible for the first time step. Therefore, the Matsuno forward time differencing scheme is used for the initial time step of each 6-hour integration cycle. This time step not only reduces solution separation but also selectively dampens high frequency waves (Haltiner, 1971). The finite difference equation for the Matsuno scheme is:

$$F^{*} = F^{t} + \Delta t \frac{\partial F^{t}}{\partial t}$$

$$F^{t+1} = F^{t} + \Delta t \frac{\partial F^{*}}{\partial t}$$

A time step of ten minutes was used for all experiments. This large time step is computationally stable when the Arakawa technique (Langlois and Kwok, 1969) of averaging quantities involved in the longitudinal derivatives is used. Without this averaging technique, the von Neumann linear computational stability criterion (Haltiner, 1971) would require a 2.5 minute time step because the longitudinal grid distance at 85° north and south is only 47 kilometers. No averaging was done equatorward of 60° north and south.

It should be noted at this time that lateral diffusion, friction, convective adjustment, convective condensation and large scale condensation are computed at every time step while heating is computed every 6 time steps (Kesel and Winninghoff, 1972).

III. INITIAL CONDITIONS

Both real and analytic data were used for initialization. The data was produced external to the main program on a Northern Hemispheric FNWC 63 x 63 grid. The analytic data with known phase propagation properties was produced following the work of Neamtan (1946), Gates (1962) and Heburn (1972). The real data was read from FNWC tapes. These fields were analyzed by the FNWC objective schemes.

The main program was used to interpolate the data so that values at 5° latitude-longitude intersections were available over the Northern Hemisphere. The data was then reflected into the Southern Hemisphere. This procedure allows for an excellent test of the program. The model begins with fields which are mirror images of each other and they should remain so. In all cases, the input data consisted of the temperature analyses for the Northern Hemisphere at 12 constant pressure levels distributed from 1000 to 50 mb, height analyses at 10 of these levels, moisture analyses at 4 levels from the surface to 500 mb, sea level pressure and sea surface temperature. Monthly mean surface temperature fields were used to derive an albedo field (Dickson and Posey, 1967). The terrain height, in the real data case, was that used by the current FNWC model. The terrain height, in the analytic data cases, was set to zero.

In order to isolate and evaluate certain numerical errors, it was decided to use analytic initial conditions for the stream function ψ, from which the true solution of the complete vorticity equation in two dimensions could be obtained. With the assumption of nondivergent horizontal flow, harmonic wave solutions of the complete vorticity equation have been obtained for the sphere by Neamtan (1946). These solutions yield the velocity of propagation of the waves. The solution for the ψ field was found to be

$$\psi = A \sin(m\lambda - \nu t)\, P_n^m(\sin\theta) - B r^2 \sin\theta + C P_n(\sin\theta) \tag{1}$$

where A, B and C are constants to be determined, r is the radius of the earth, m is the hemispheric wave number, ν/m is the angular phase speed of the wave disturbance (radians / second), P_n denotes the Legendre polynomial and P_n^m represents the associated Legendre function.

If we choose C = 0 (Gates, 1962) and n = m + 1 [Buringt n and Torrance (1936), Kreyszig (1962)] equation (1) reduces to

$$\psi = A \sin(m\lambda - \nu t)(2N!/2^N N!) \sin\phi\ (\cos\phi)^6 - B r^2 \sin\phi\,. \tag{2}$$

The constant A is arbitrary and proportional to the wave amplitude. But it was shown by Haurwitz (1940) that the solution obtained for ψ implies the existence of a velocity distribution over the sphere such that the angular velocity of the westerly current is made up of the sum of three terms.

The first term, B, is constant over the sphere; the second term varies along a meridian but is constant round a circle of latitude; and the third term represents a harmonic wave which is propagated zonally with a constant angular velocity, ν/m, which is given by the formula

$$\nu/m = B\,\frac{n(n+1) - 2}{n(n+1)} - \frac{2\Omega}{n(n+1)} \qquad (3)$$

where Ω is the earth's rotation speed.

A reasonable meteorological pattern was obtained by choosing A as 1000 $m^2 sec^{-1}$, m as 6 and ν/m as -13°, 0° and +12° longitude per day respectively. The ψ field thus obtained was used to determine the initial fields.

The geopotential fields were derived by solution of the linear balance equation

$$\nabla^2 \phi = [f\,\nabla^2\psi + \nabla\psi \cdot \Delta f] \qquad (4)$$

over the entire Northern Hemisphere. Equation (4) was solved using the over-relaxation iterative technique with a relaxation tolerance of one meter (Haltiner, 1971).

The temperatures generated for the analytic cases were constant over each pressure surface and were consistent with the National Advisory Committee for Aeronautics (NACA) standard atmosphere (Haltiner and Martin, 1957). The elevation 10,769 meters represents the tropopause in this

atmosphere. The following relations were used in calculating the analytic temperatures.

$$T_P(°K) = 288 - 0.0065\ Z \qquad Z \leq 10{,}769 \text{ meters}$$

$$T_P(°K) = 218 \qquad Z \geq 10{,}769 \text{ meters}$$

$$Z_P(m) = 44{,}308\ [1 - (\frac{P}{1013.25})^{0.19023}] \qquad Z \leq 10{,}769 \text{ meters}$$

$$Z_P(m) = 10{,}769 + 6381.6\ \ln(\frac{234.52}{P}) \qquad Z \geq 10{,}769 \text{ meters}$$

In the foregoing equations, the pressure is in millibars and the height Z, is in meters. In addition, the specific humidity (q) at the lowest three levels was set to zero and the forecast procedure excluded friction, convection adjustment, large scale convective condensation, large scale condensation, heating and terrain influences.

The initial wind fields in the analytic cases were obtained in two ways. Winds obtained analytically from the original ψ fields were called "analytic winds." Winds obtained from the linear balance equation were called "derived winds." It should be noted that "derived winds" were used for the real data case.

A. ANALYTIC WINDS

The initial wind fields for the "analytic wind" cases were derived directly by differentiation of the initial

ψ field (Neamtan, 1946). The formulas for the non-divergent wind components are

$$u = -\frac{1}{a}\left\{A \sin(m\lambda-\nu t)\left(\frac{2N!}{2^N N!}\right)[(\cos\theta)^7 - 6(\sin\theta)^2(\cos\theta)^5] - B r^2 \cos\theta\right\} \quad (5)$$

$$v = \frac{1}{a} A \left(\frac{2N!}{2^N N!}\right) \sin\theta (\cos\theta)^6 m \cos(m\lambda-\nu t) \quad (6)$$

where a is the earth's radius, A is an arbitrary constant that is proportional to the wave amplitude, θ is the latitude, ν is the angular velocity of the wave, λ is the longitude, m is the wave number and N = m+1.

B. DERIVED WINDS

The "derived wind" field was obtained from a ψ field using the finite difference expressions

$$u = -\frac{1}{a}\frac{\Delta\psi}{\Delta\theta}$$

and

$$v = \frac{1}{a\cos\theta}\frac{\Delta\psi}{\Delta\lambda}$$

where a is the earth's radius, $\Delta\theta$ is the latitudinal distance increment and $\Delta\lambda$ is the longitudinal distance increment. The ψ and ϕ fields were obtained in two parts

depending on latitude. Poleward of 25° north and south, the initial* geopotential field, say ϕ_o, was retained and the ψ field was obtained by solution of the linear balance equation

$$\nabla^2\psi + \nabla\psi\cdot\nabla f/f = \nabla^2\phi_o/f \quad .$$

Equatorward of 25° north and south, the field was determined using

$$\psi = \phi_o/\overline{f}$$

where $\overline{f}$ is a mean coriolis parameter. Then a new geopotential field (ϕ) was obtained by solution of the linear balance equation

$$\nabla^2 = (f\nabla^2\psi + \nabla\psi\cdot\nabla f) \quad .$$

At 25° north and south, ψ and ϕ were a combination of half the ψ and ϕ from the poleward case and half the ψ and ϕ from the equatorward case. It was hoped that this would reduce the amplitude of the high frequency oscillations in the tropics (Winninghoff, 1971).

---

*By initial geopotential field is meant either the FNWC objective analysis of ϕ or a simulated ϕ field-obtained by solution of Equation (4) using the analytic function form of ψ (Equation (1)).

IV. WAVE ANALYSIS METHOD

A Fourier series was determined at each five degrees of latitude around the latitude circle. The employment of such a series, known as harmonic analysis, is extensively used in the study of observational data (Jeffreys and Jeffreys, 1956). With this technique, the phase angles and amplitudes of each wave number around a latitude circle can be calculated. A Fourier series can be expressed as follows (Heburn 1972):

$$F(x) = A_o + \sum_m (A_m \cos mx + B_m \sin mx)$$

$$= C_o + \sum_m (C_m \cos (mx - \delta m)$$

where

$$C_m = \frac{B_m}{\sin(\delta m)} = \frac{A_m}{\cos(\delta m)}$$

and

$$\delta_m = \tan^{-1}(\frac{B_m}{A_m}).$$

The first three experiments involved an input stream function of wave number six. The values of primary interest, therefore, were δ_6 and C_6 which are the phase angle and amplitude of wave number six. Other phase angles and amplitudes were extracted and examined, especially in the real data case.

V. RESULTS

Four experiments will be presented in this section. The first three of these experiments were performed with analytic fields. These analytic fields were derived from a stream function with a wave number of 6 and arbitrary constant, A, set equal to 1000 $m^2 sec^{-1}$. The vertical temperature structure of these fields was determined by the NACA standard atmosphere. Experiments I and II consisted of two 36-hour forecasts each. The first forecast used "analytic" winds and the second forecast "derived" winds. Experiment III consisted of one 36-hour forecast using "analytic" winds. Experiment IV was performed with FNWC analyses and consisted of one 36-hour forecast using "derived" winds.

Experiment I. The analytic geopotential field used in this experiment was derived from a stream function with a wave number of 6 and phase speed of -13° longitude per day. The initial surface pressure analysis is shown on chart E. The forecast surface pressure fields using both "analytic" and "derived" winds can be found on charts F-H.

Experiment II. The analytic geopotential field used in this experiment was derived from a stream function with a wave number of 6 and phase speed of 0° longitude per day. The initial surface pressure analysis is shown on chart I. The forecast surface pressure fields using both "analytic" and "derived" winds can be found on charts J-L.

Table I compares the wave amplitudes and mean heights of the 36-hour forecast pressure field for experiment II (analytic winds) with those of the initial pressure field at selected latitudes. The amplitudes and mean heights in this experiment decreased at latitudes equatorward of 30° north (south) and increased poleward of 30° north (south). These amplitude variations are believed to be caused by nonlinear effects.

In addition, Figures 6 - 8 are plots of terrain pressure versus forecast hour at selected latitudes. These terrain pressures are plotted every hour out to 36 hours. They show small amplitude internal gravity waves with periods ranging from 6-12 hours. These oscillations are believed to be due to the geostrophic adjustment mechanism and are peculiar to the type of analytic field used.

Experiment III. The analytic field used in this experiment was derived from a stream function with a wave number of and a phase speed of 12° longitude per day. The initial surface pressure analysis is shown on chart M. The forecast surface pressure fields using "analytic" winds only can be found on charts N-P.

Experiment IV. This experiment was performed using FNWC objective analyses for 00Z February 8, 1973. The initial surface pressure analysis is shown on chart A. The surface pressure analysis for 12Z February 8, 1973 is shown on chart B. The 12-hour forecast made by the current FNWC

model is shown on chart C. The 12-hour forecast made by the global model is shown on chart D.

It should be noted that Experiment IV included terrain, frictional stress, heating and moisture effects as discussed in Kesel and Winninghoff (1972).

Table II summarizes the results of all experiments performed. The analytic phase speeds are compared to the actual phase speeds for all experiments using analytic data. The table also includes A which is proportional to the amplitude of the analytic wave, B which is a function of the phase speed and wave number, the method of balancing and the time required to make a 36-hour forecast.

The forecast fields in all the experiments using analytic data showed a considerable tilt backward at high latitudes in the phase propagation of the wave. This was to be expected since the Arakawa averaging technique tends to smooth the gradients at high latitudes. In addition, the Arakawa technique gives an effective Δx which is comparable to that at low latitudes, thus as the wavelength decreased toward the poles the phase speed also decreased (Gates, 1959).

The result of this differential movement, which was more pronounced in the "derived" wind cases, was the formation of closed highs and lows at the higher latitudes which propagated equatorward. This distortion was aggravated by nonlinear effects introduced after the field ceased to be harmonic in the longitudinal direction.

Furthermore, in all the experiments using the "derived" wind, high frequency inertial gravity waves were generated due to the initial imbalance between the mass and wind fields in the tropics. These gravity waves caused a rapid deterioration of the harmonic six-wave pattern and added appreciably to the problem at the poles. The shear which developed at 25° north (south) was attributed to the method used to blend the winds between the tropics and mid-latitudes. The larger error in the phase speeds calculated for the "derived" wind cases were also attributed to this initialization.

Since these experiments were performed using a multi-level primitive equation model which allows divergence, Equation (3) was satisfied only approximately. Also, Rossby (1939) has shown that the presence of divergence in a barotropic atmosphere will slow the rate of wave propagation, especially for small values of wave number. It was not surprising, therefore, that the actual phase speed was always less than expected.

Finally, a thorough examination was made of Experiment IV to determine the general quality of the program, that is, if the inertial-gravity motions were being controlled realistically so that the model produces consistent meteorological appearing results. Figures 3 - 5 give the surface pressure oscillations at each hour of a 36-hour forecast for selected latitudes using the full global model. In addition, Table III compares forecast pressures of the global model to both the verifying analysis and forecasts

made by the FNWC model for selected lows and highs. In interpreting these results one should keep in mind the crude initialization. Also, for those not accustomed to seeing values of terrain pressure at each hour in a primitive equation model, these oscillations, although larger than normal at these points, are by no means unusual for such a poorly initialized integration. There is no artificial smoothing done and recall that the run begins with a linear balance wind. In addition, there are none of the various devices which operational experience has shown is necessary to give an acceptable short term product, i.e., not calling on convective adjustment for the first several time steps. Nevertheless, these results are stable and retain the dominant meteorological scale without difficulty.

TABLE I

Latitudes	Amplitude of Wave #6 (C_6)		Mean Pressure (C_1)	
	Initial Pressure Field	36-Hour Forecast Pressure Field	Initial Pressure Field	36-Hour Forecast Pressure Field
Equator	5.4	4.4	1051	1040
10° N	18.2	11.0	1035	1034
20° N	29.1	24.0	1016	1015
30° N	30.2	30.2	995	995
40° N	21.5	25.5	973	977
50° N	10.1	15.0	953	956
60° N	2.7	5.8	935	937
70° N	.31	1.5	922	924
80° N	.01	.37	914	919

Note: Data is from Experiment II (Analytic Winds)

TABLE I. Wave Amplitude and Mean Heights for Selected Latitudes and Forecast Time.

TABLE II

Experiment Number	Analytic Phase Speed (°long/day)	A	B	Wave Number	Method of Balancing	Time Required For 36 Hour Forecast (Minutes)*	Actual Phase Speed For 36 Hours (°long/day)			
							Eq	30°N	60°N	75°N
I	-13	1000	0	6	Analytic Winds	108	-8	-9	-12	-18
I	-13	1000	0	6	Derived Winds	109	+3	-9	-15	-23
II	0	1000	2.7×10^{-6}	6	Analytic Winds	105	-1	+1	-1	-9
II	0	1000	2.7×10^{-6}	6	Derived Winds	106	-1	-3	-3	-12
III	+12	1000	5.2×10^{-6}	6	Analytic Winds	105	+9	+11	+7	0
IV	--	--	-	-	Derived Winds	135				

*Time is in CPU minutes on a 6500 CDC Computer. It includes all diagnostic routines such as Fourier series analysis, interpolations, etc.

TABLE II. Computed Phase Speeds at Selected Latitudes Along with Method of Balancing and Time Required to Make a 36-Hour Forecast for each Experiment

TABLE III

Location of Pressure System on Initial Surface Analysis	Initial Surface Pressure Analysis 00Z 8 Feb 1973	Verifying Surface Pressure Analysis 12Z 8 Feb 1973	FNWC 12-hour Surface Pressure Analysis	Global 12-hour Surface Pressure Analysis
65°N 135°W	1042(H)	1041	1040	1042
70°N 15°E	971(L)	975	976	973
65°N 25°W	991(L)	990	989	989
65°N 70°W	999(L)	992	992	992
50°N 165°E	966(L)	962	959	962
55°N 115°E	1049(H)	1046	1043	1052
55°N 45°E	974(L)	976	975	975
50°N 55°W	1031(H)	1030	1029	1036
50°N 100°W	1037(H)	1037	1037	1040
50°N 160°W	1004(L)	1009	1004	1005
35°N 175°W	1030(H)	1030	1029	1031
30°N 20°W	1006(L)	1009	1007	1003
35°N 55°W	1012(L)	1006	1007	1010

TABLE III. Comparison of 12-Hour Forecast Pressures of the FNWC Model and the Global Model Against the Verifying Pressure Analysis (Experiment IV).

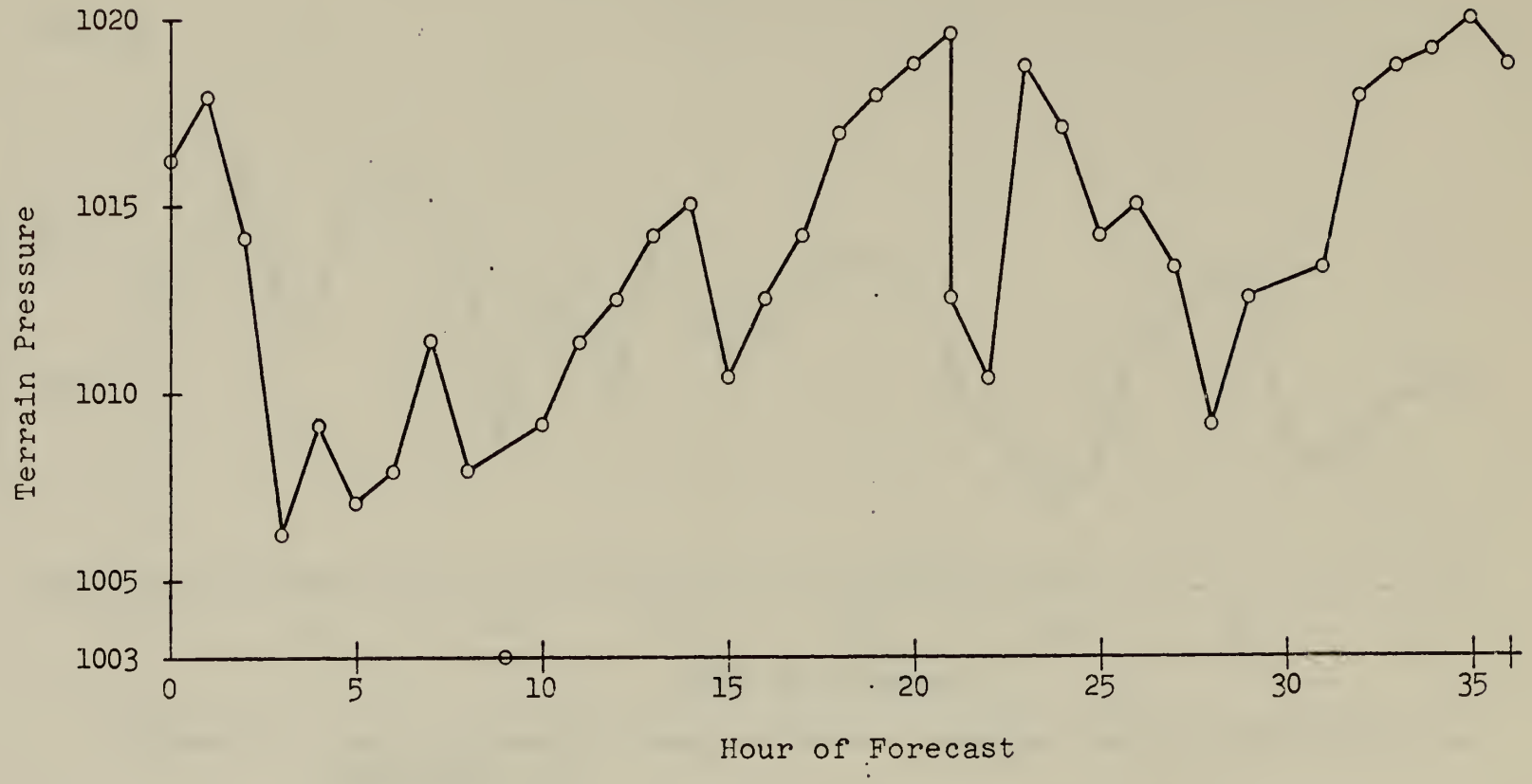

Figure 3. Plot of Terrain Pressure Versus Forecast Hour at 15°E 0°N for Experiment IV

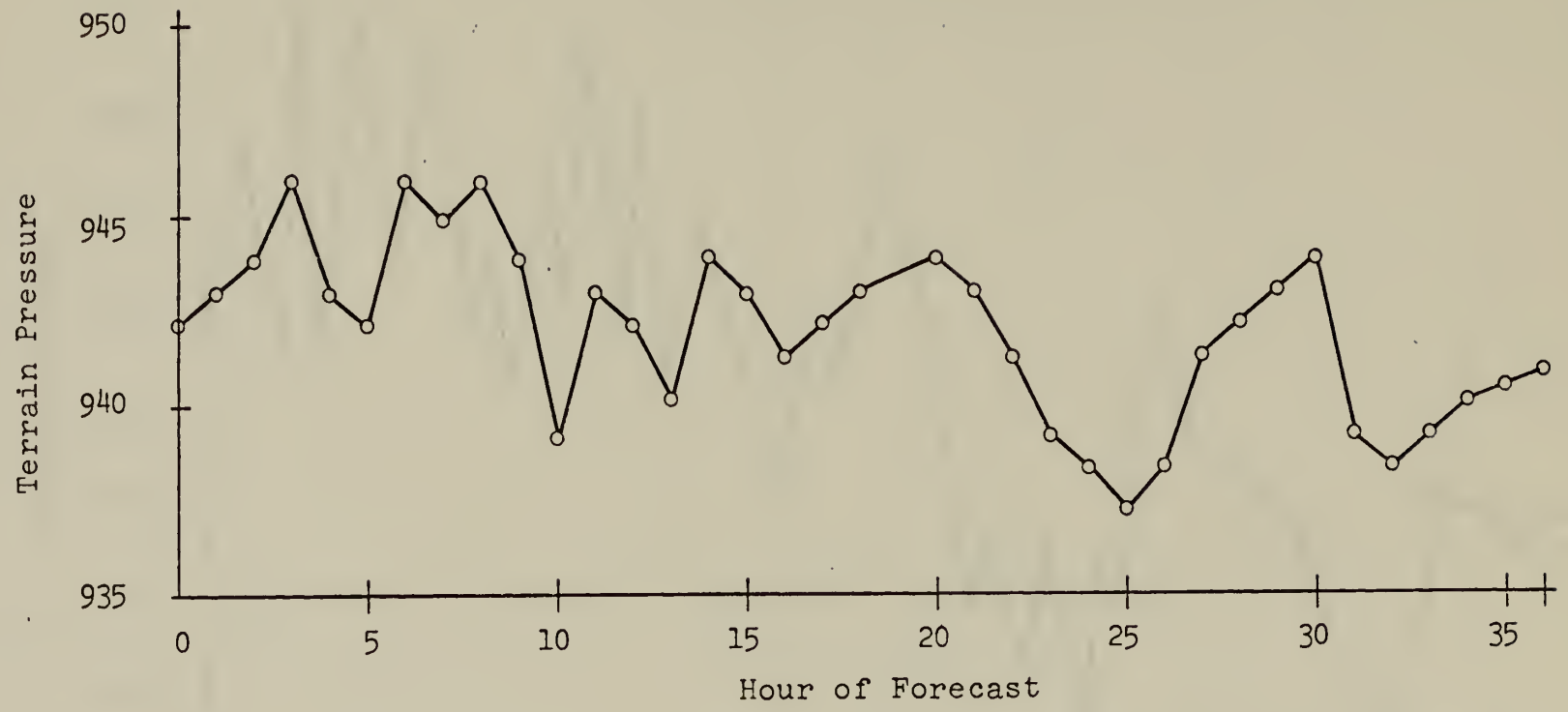

Figure 4. Plot of Terrain Pressure Versus Forecast Hour at 15°E 40°N for Experiment IV.

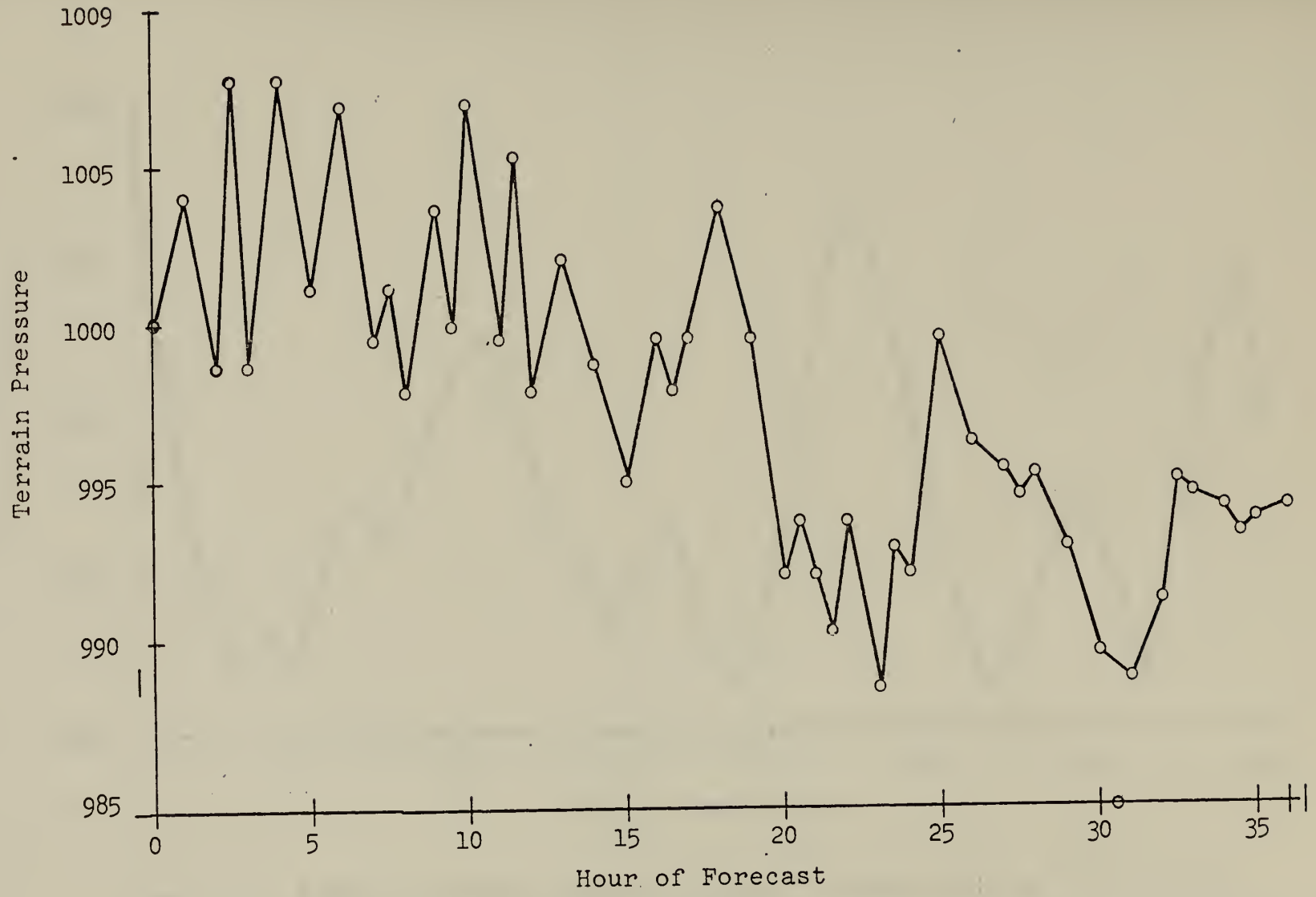

Figure 5. Plot of Terrain Pressure Versus Forecast Hour at 15°E 85°N for Experiment IV.

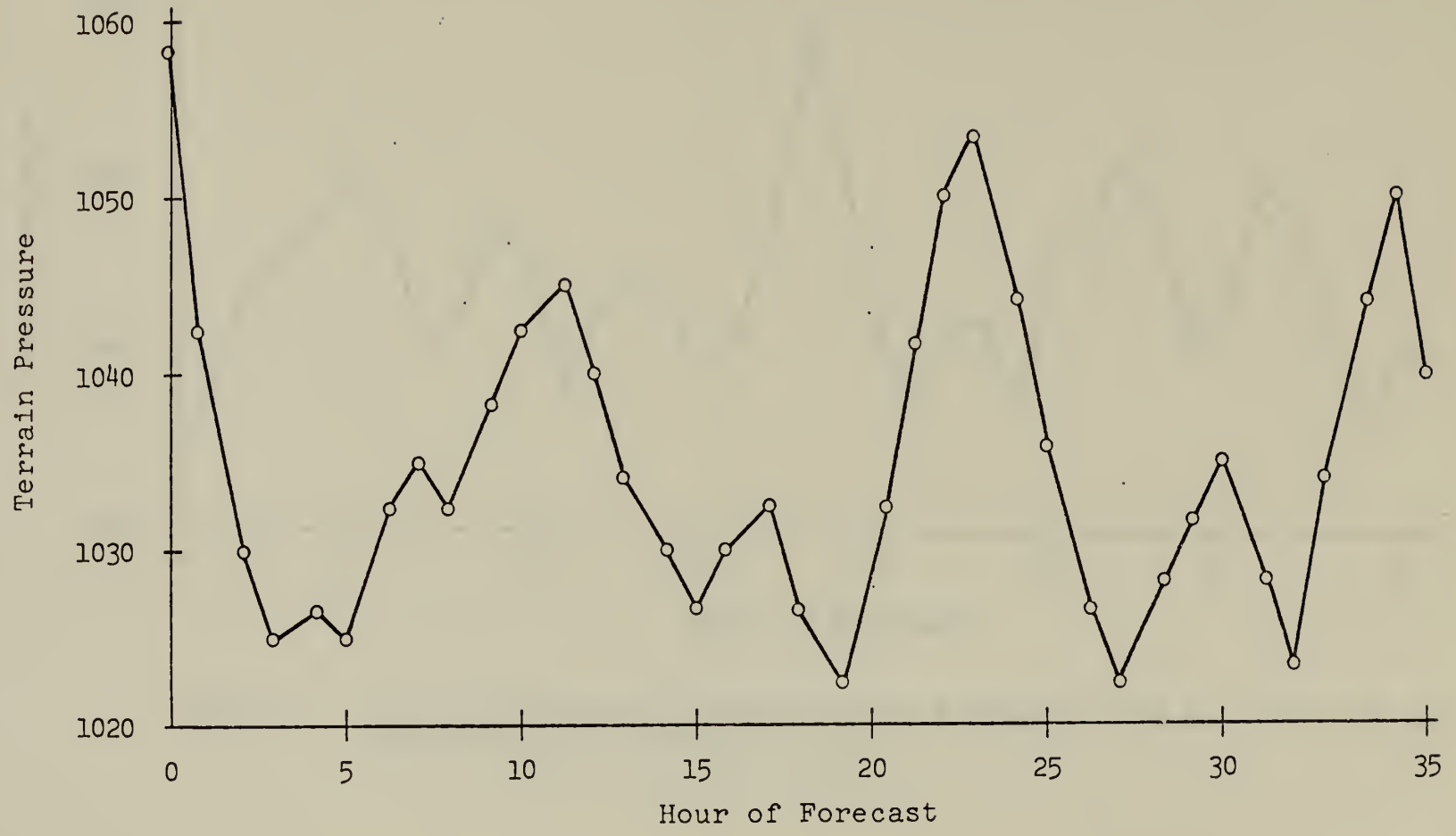

Figure 6. Plot of Terrain Pressure Versus Forecast Hour at 15°E 0°N for Experiment II (Analytic Winds).

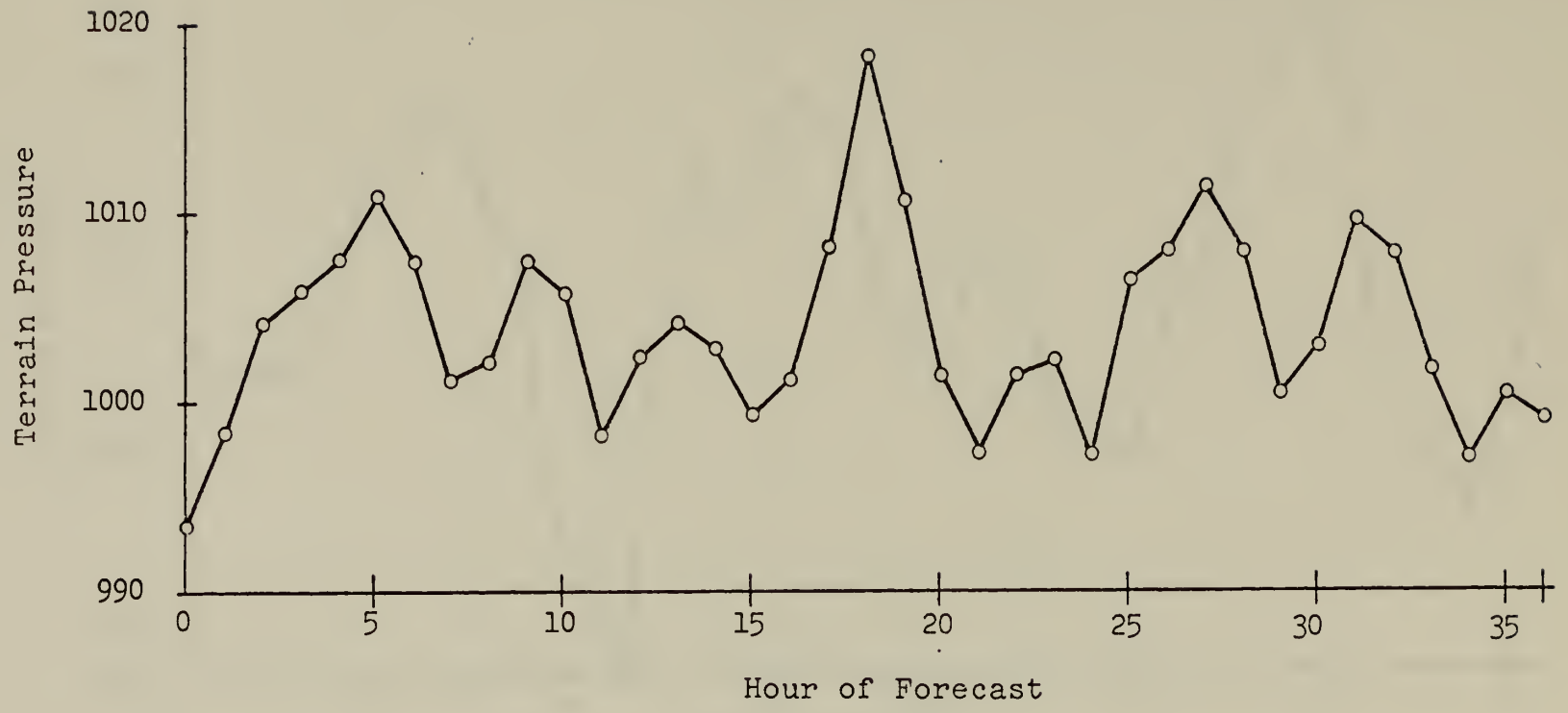

Figure 7 . Plot of Terrain Pressure Versus Forecast Hour at 15°E 40°N for Experiment II (Analytic Winds).

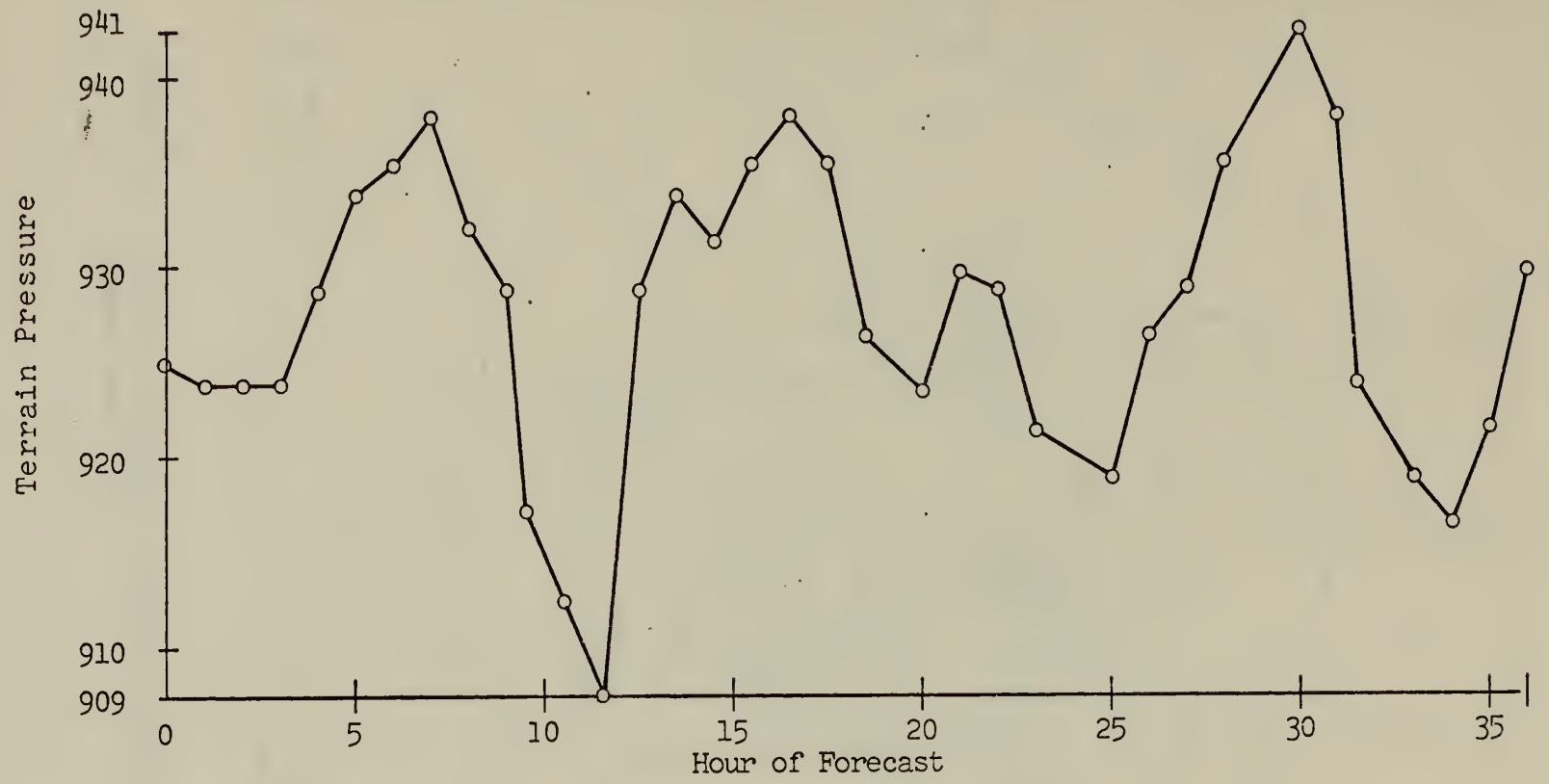

Figure 8. Plot of Terrain Pressure Versus Forecast Hour at 15°E 85°N for Experiment II (Analytic Winds)

CHART A. Initial Surface Pressure Analysis
(Experiment IV)

CHART B. Verifying Surface Pressure Analysis
(Experiment IV)

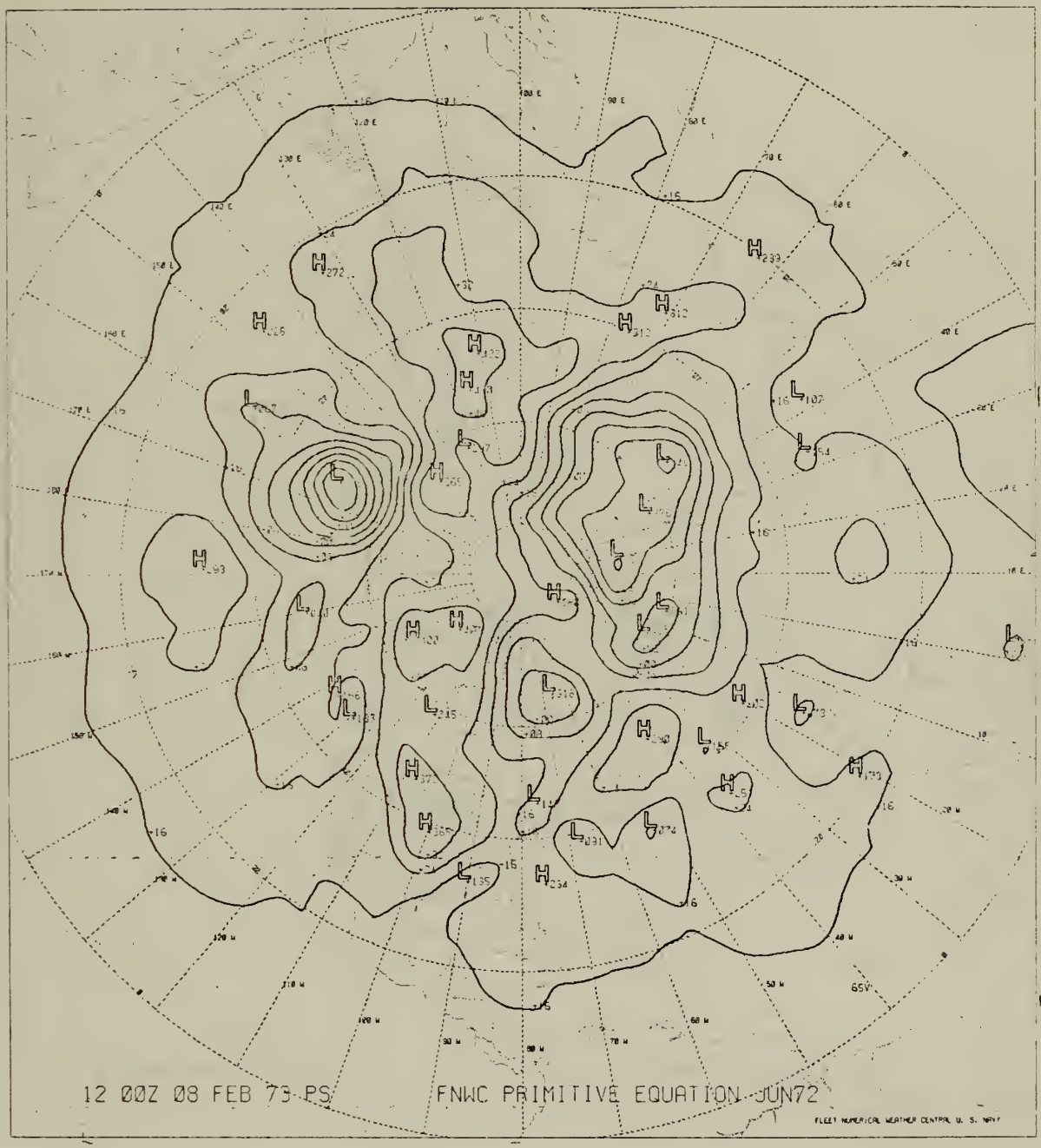

CHART C. 12-Hour Forecast Using FNWC Model
(Experiment IV)

CHART D. 12-Hour Forecast Using Global Model (Experiment IV)

CHART E. Initial Surface Pressure Analysis
(Experiment I)

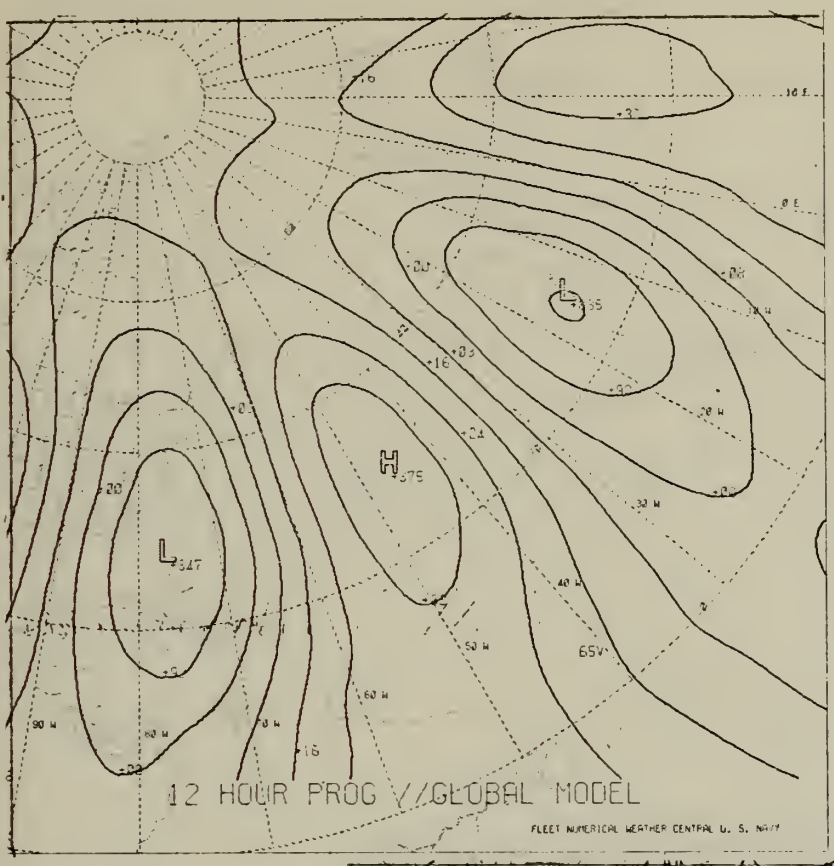

Analytic Winds

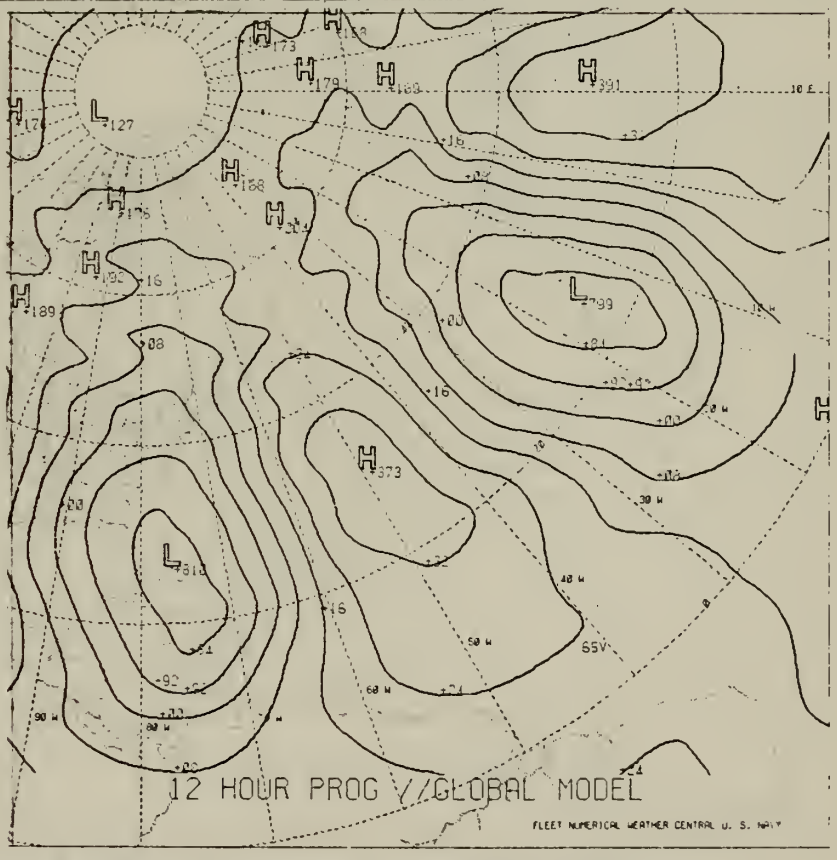

Derived Winds

CHART F. 12-Hour Surface Pressure Forecast Using Analytic and Derived Winds (Experiment I)

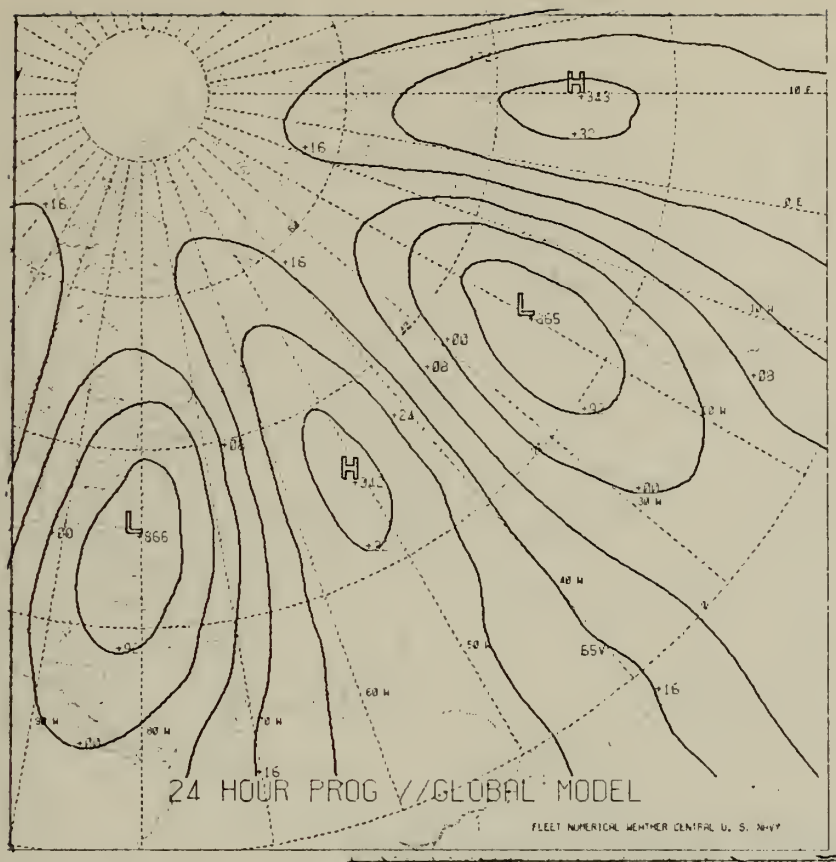

Analytic Winds

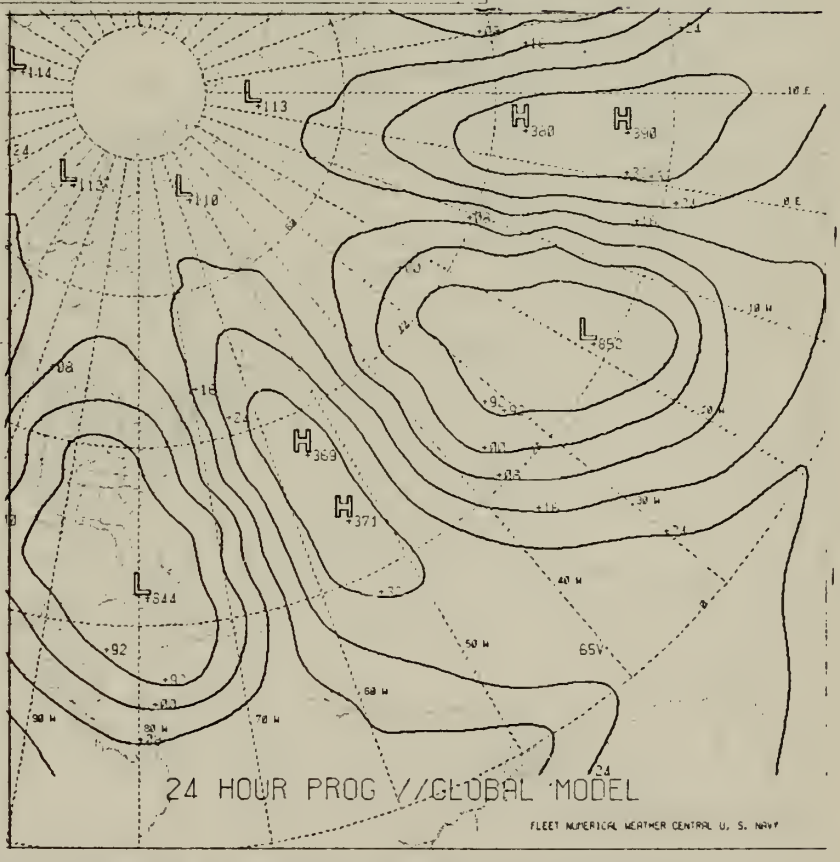

Derived Winds

CHART G. 24-Hour Surface Pressure Forecast Using Analytic and Derived Winds (Experiment I)

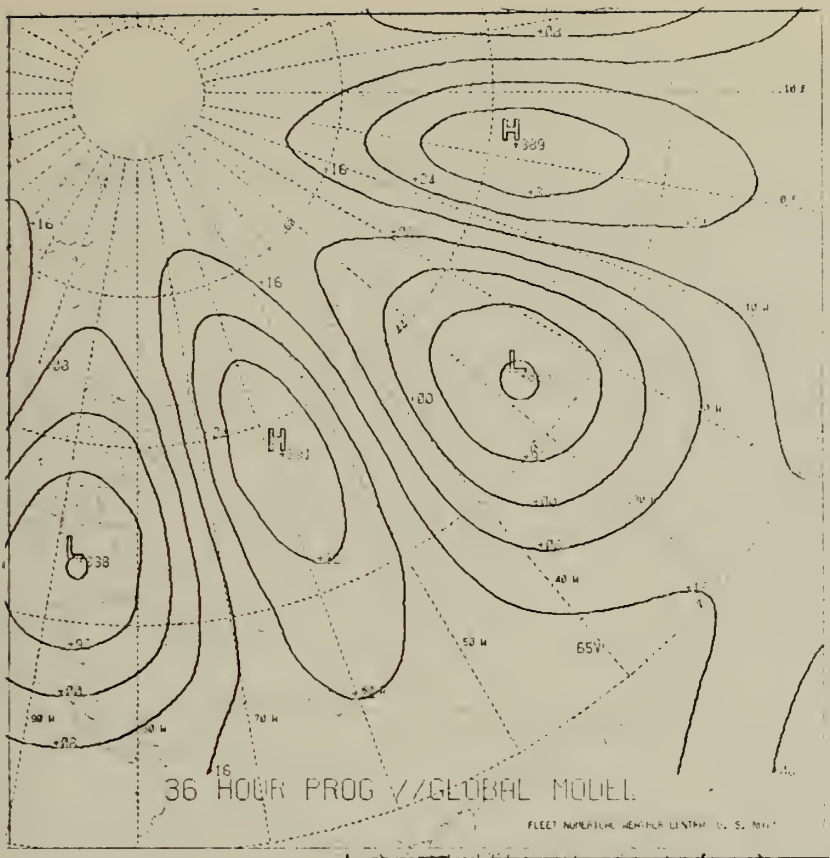

Analytic Winds

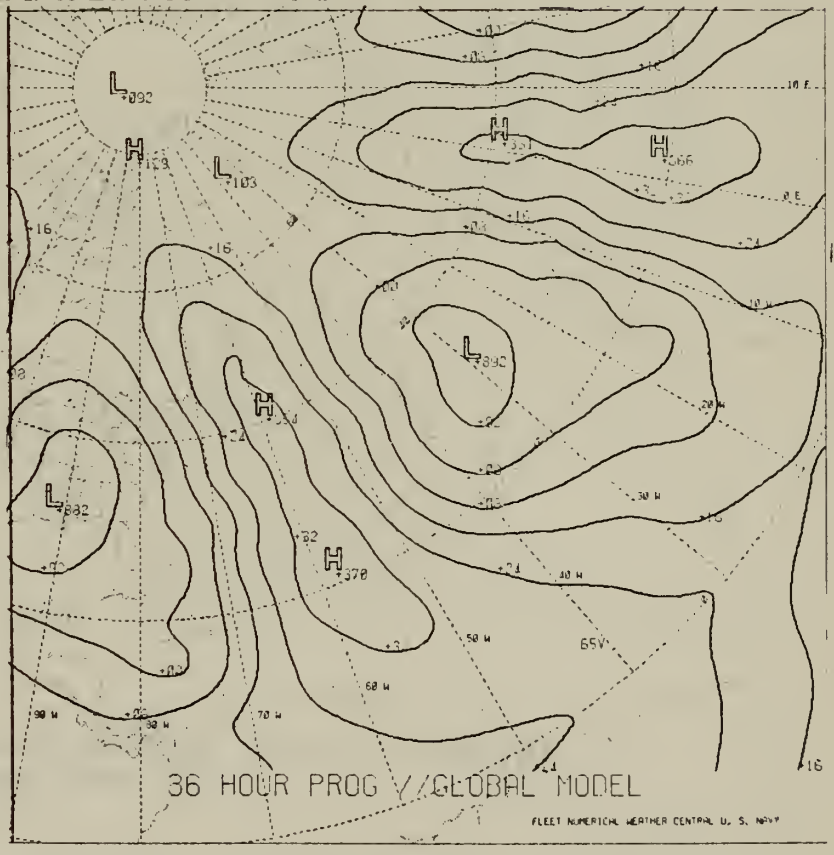

Derived Winds

CHART H. 36-Hour Surface Pressure Forecast Using Analytic and Derived Winds (Experiment I)

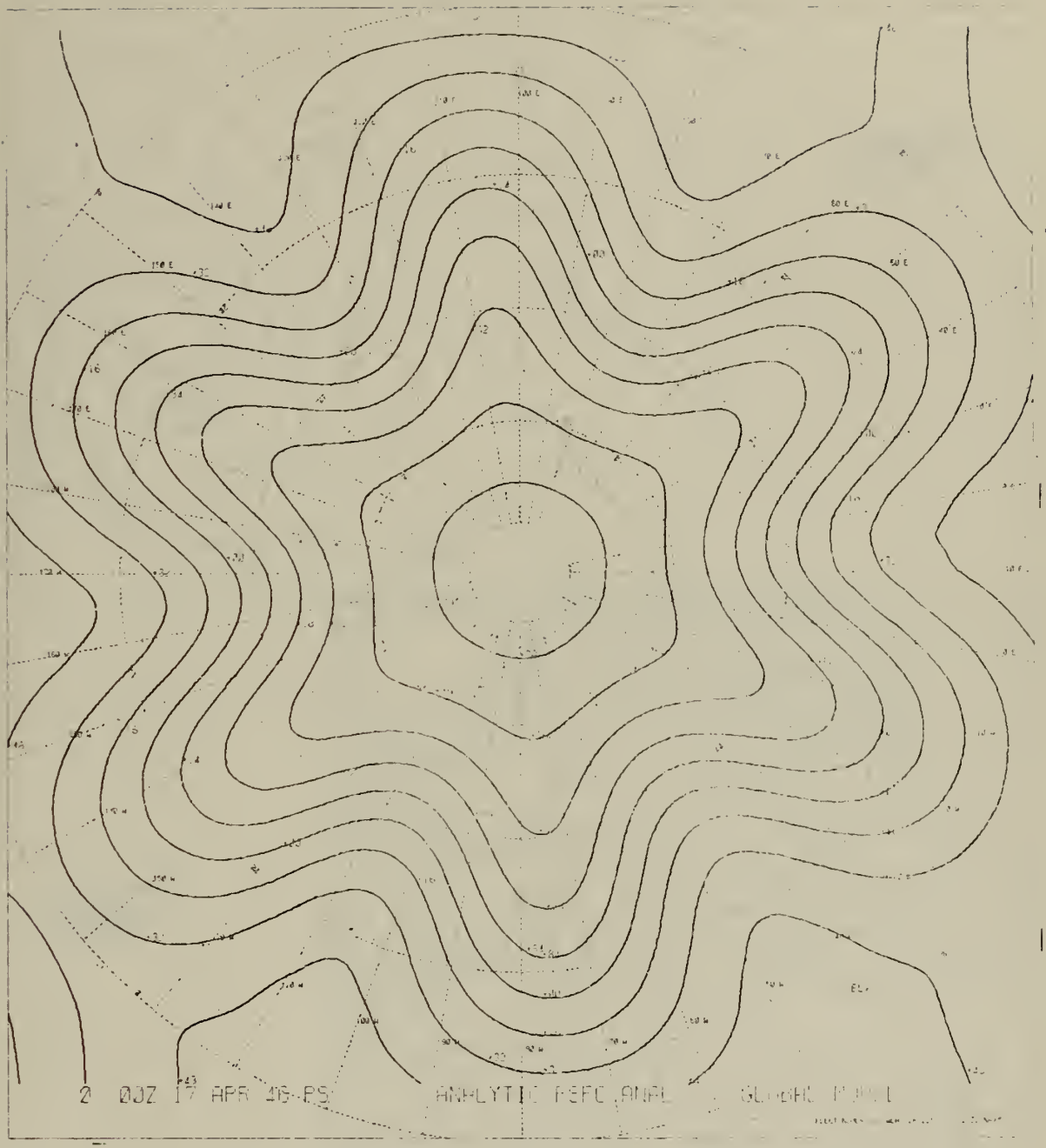

CHART I. Initial Surface Pressure Analysis
(Experiment II)

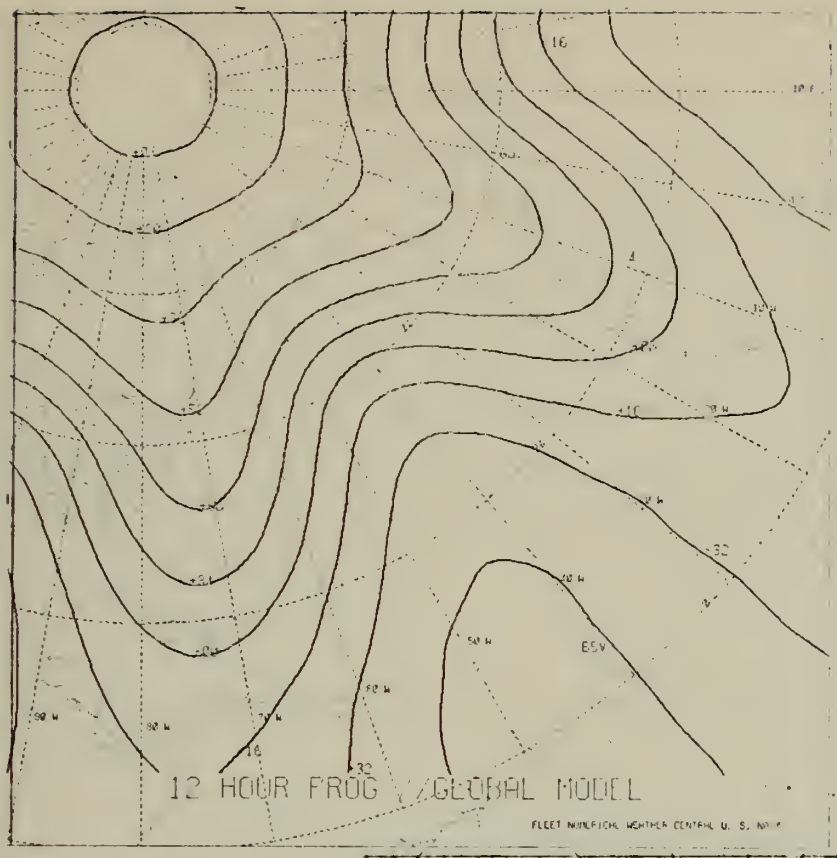

Analytic Winds

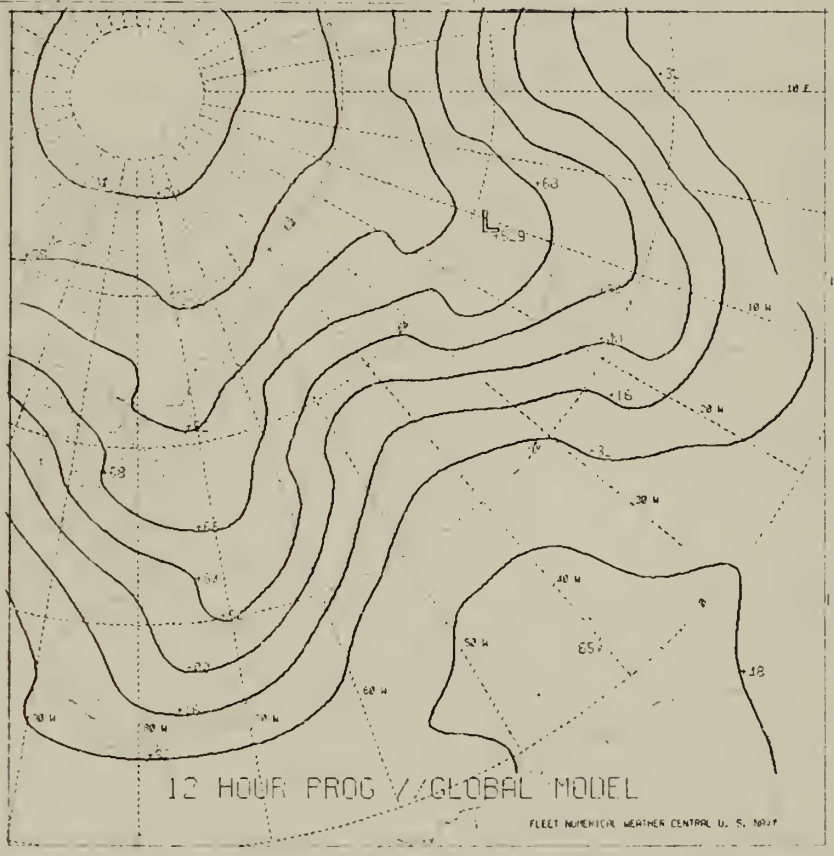

Derived Winds

CHART J. 12-Hour Surface Pressure Forecast Using Analytic and Derived Winds (Experiment II)

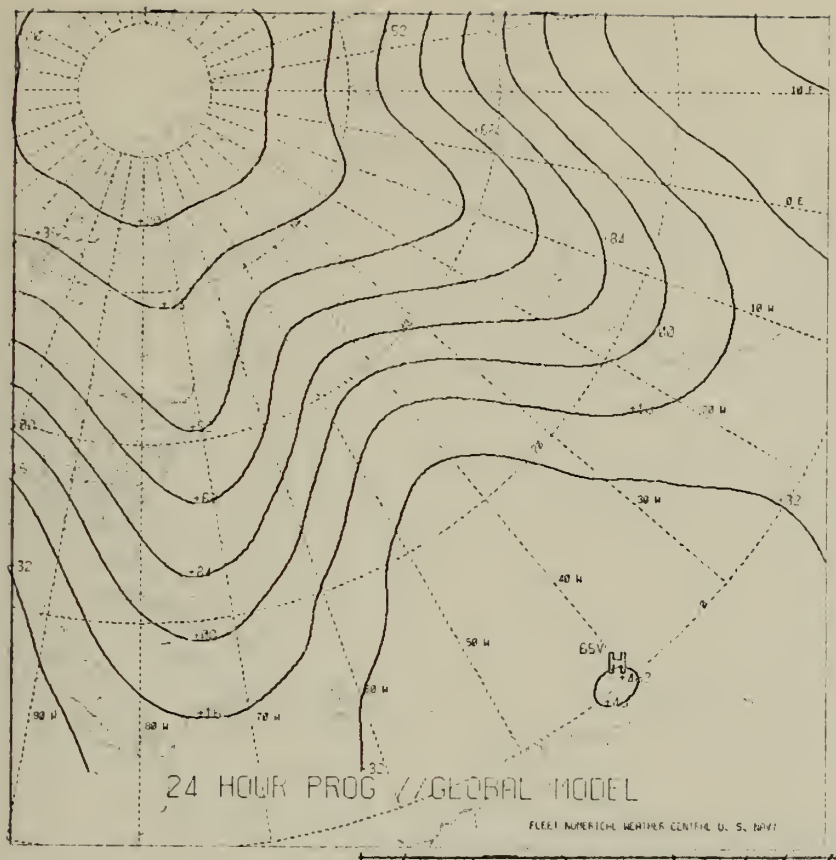

Analytic Winds

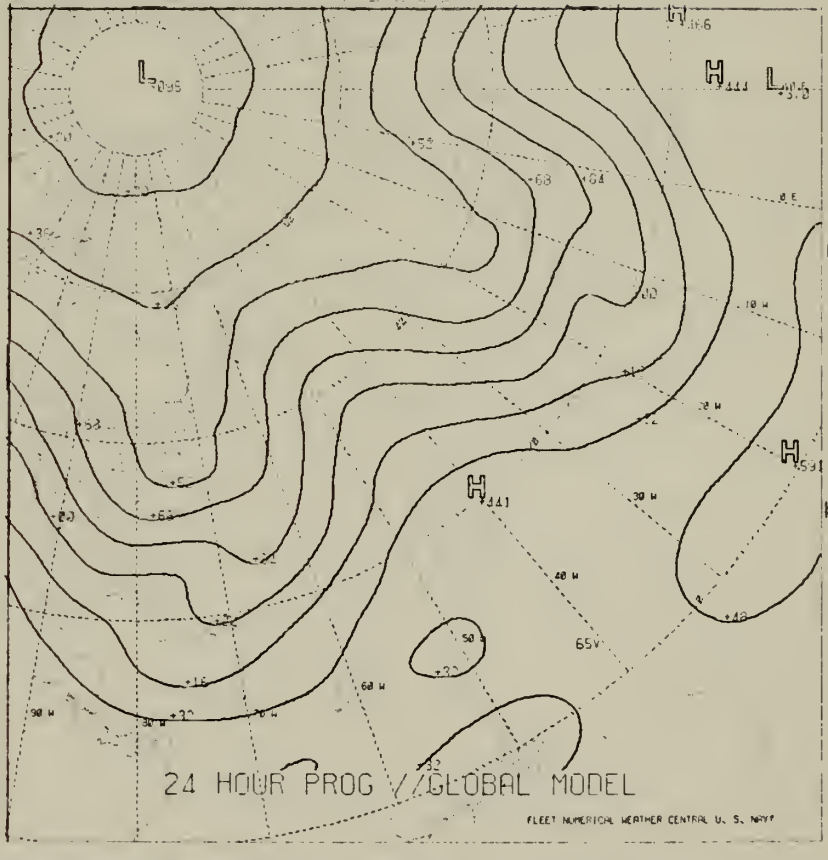

Derived Winds

CHART K. 24-Hour Surface Pressure Forecast Using Analytic and Derived Winds (Experiment II)

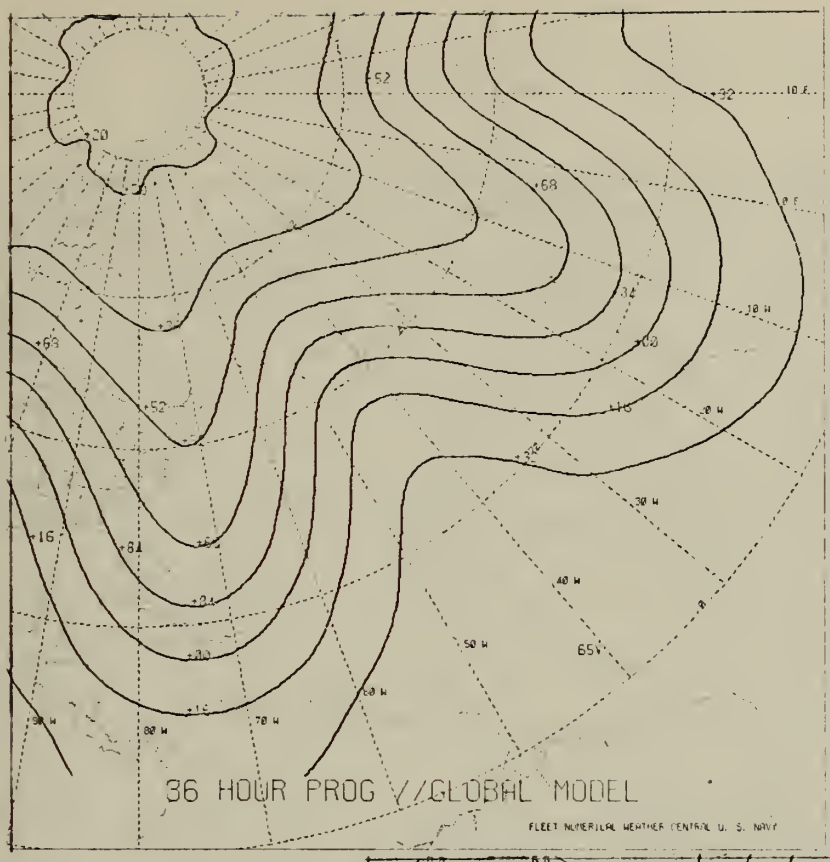

Analytic Winds

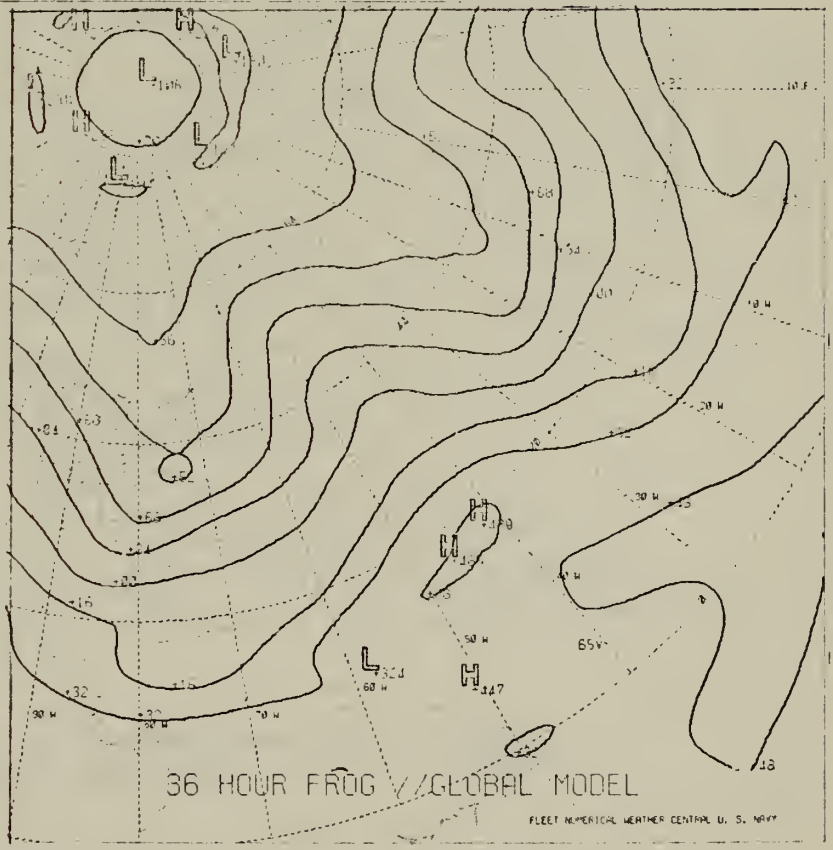

Derived Winds

CHART L. 36-Hour Surface Pressure Forecast Using Analytic and Derived Winds (Experiment (II)

CHART M. Initial Surface Pressure Analysis
(Experiment III)

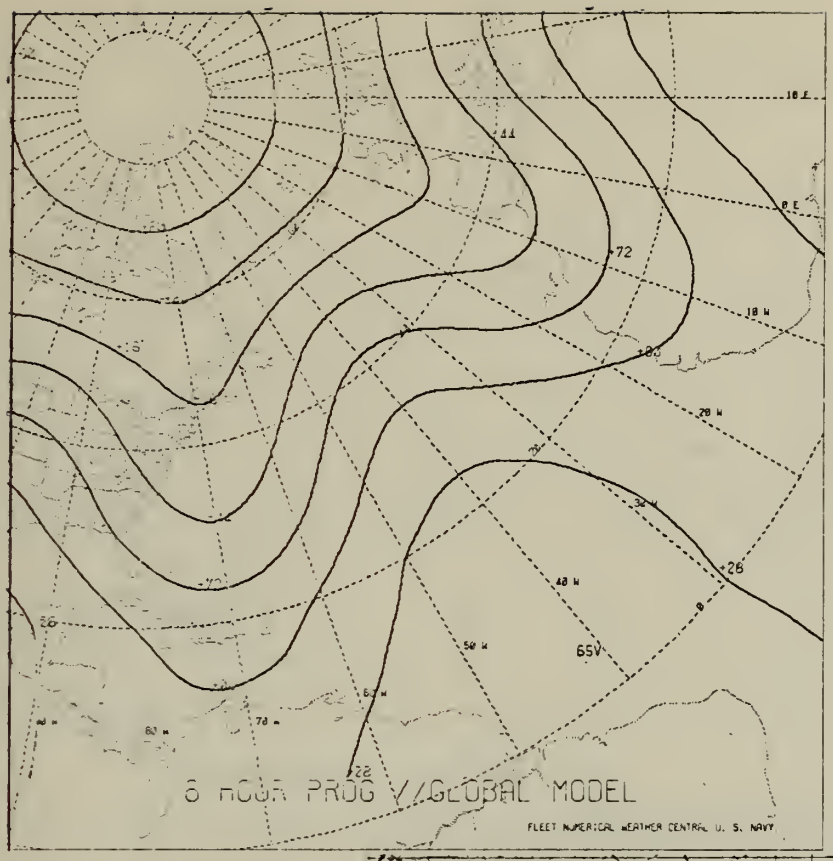

Analytic
Winds

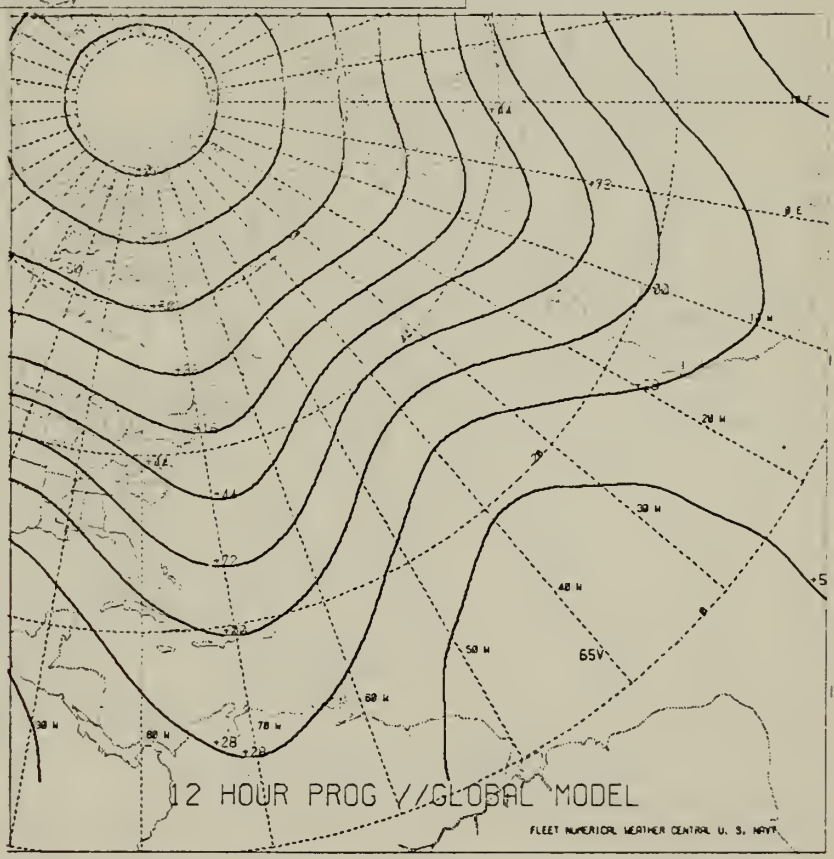

Analytic
Winds

CHART N. 6-Hour and 12-Hour Surface Pressure Forecast Using Analytic Winds (Experiment III)

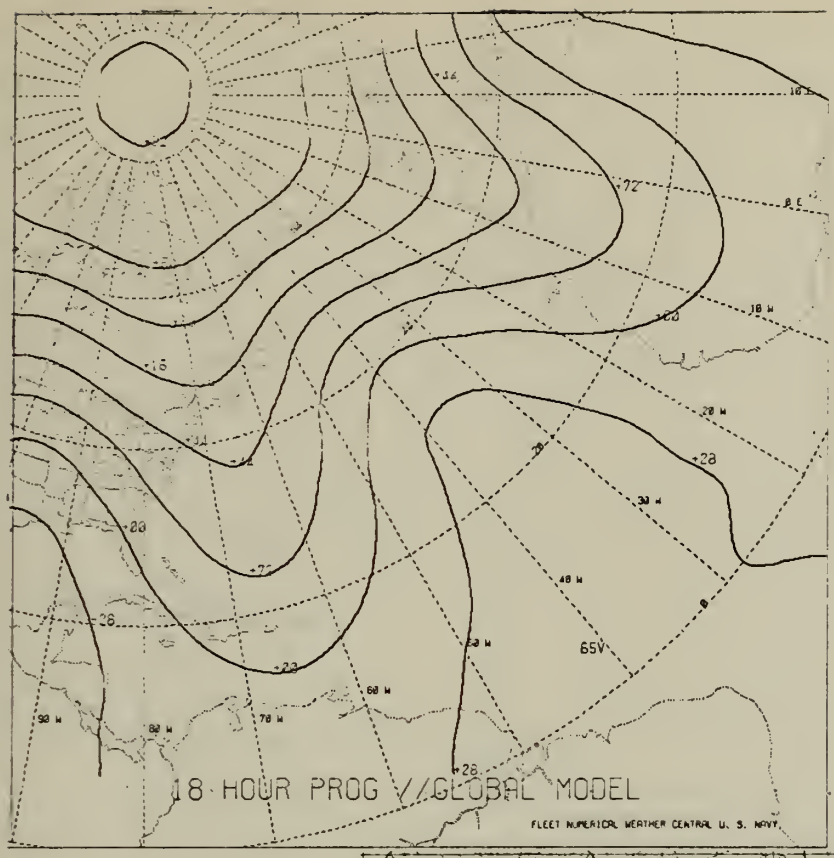

Analytic
Winds

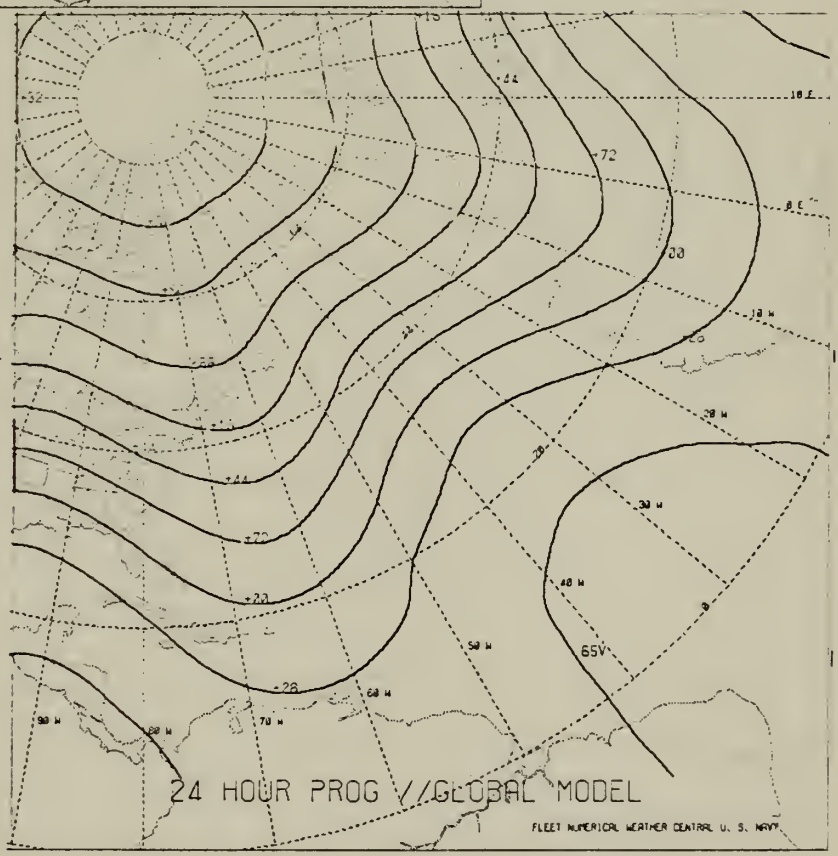

Analytic
Winds

CHART O. 18-Hour and 24-Hour Surface Pressure Forecast Using Analytic Winds (Experiment III)

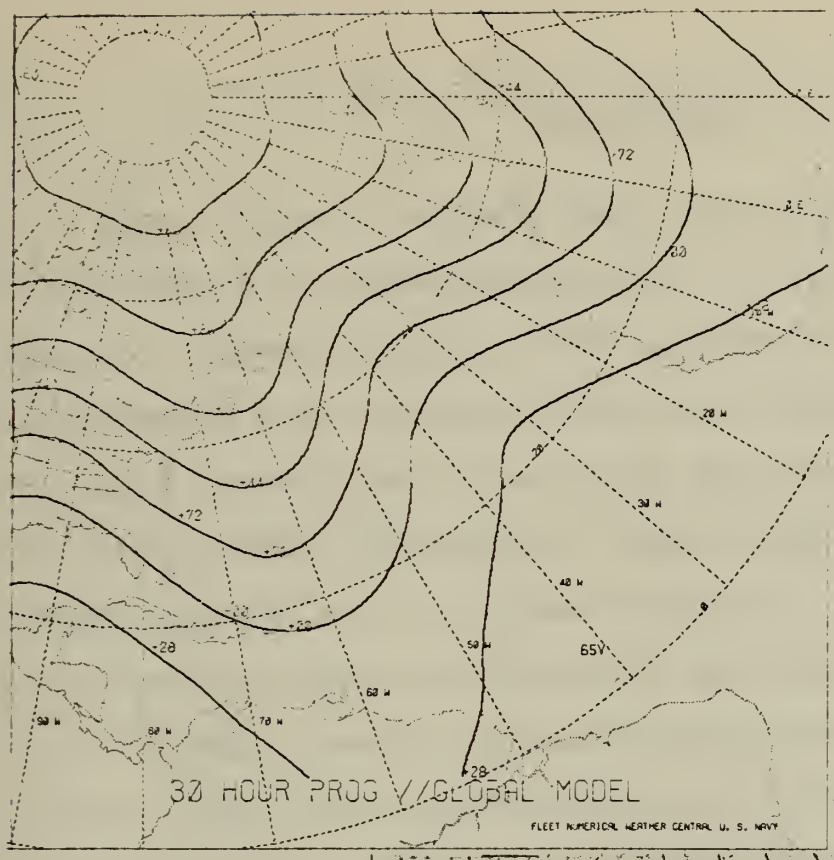

Analytic
Winds

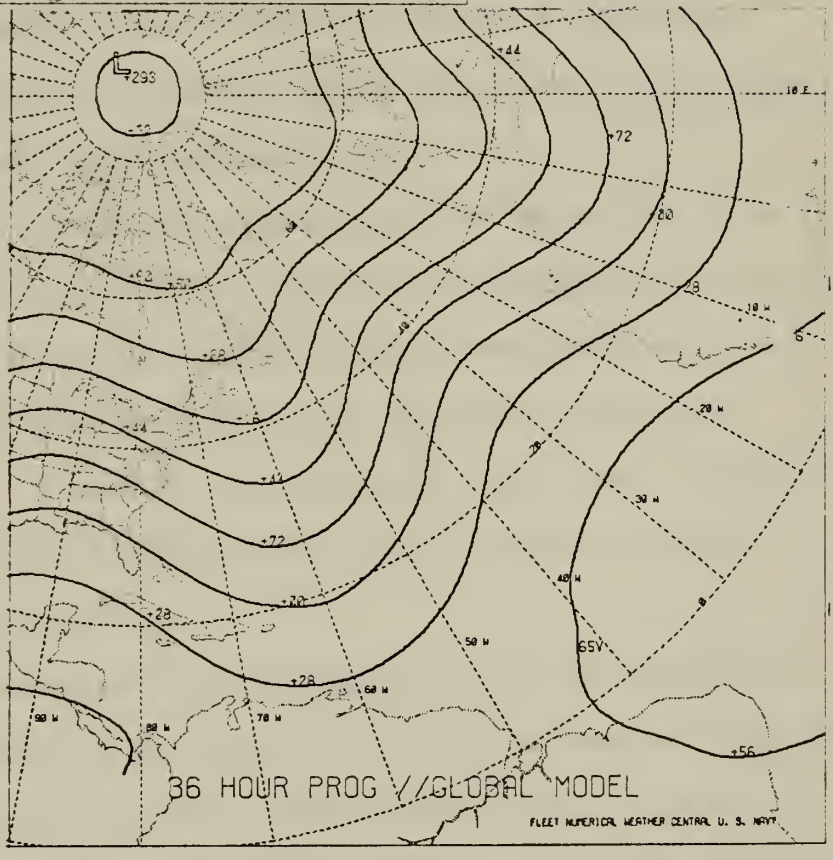

Analytic
Winds

CHART P. 30-Hour and 36-Hour Surface Pressure Forecast Using Analytic Winds (Experiment III)

VI. CONCLUSIONS

Three cases of analytic data and one case of real data were numerically integrated using a 5-level baroclinic primitive equation model of the general circulation. Experiments were performed using winds derived from the linear balance equation and winds derived analytically. The feasibility of using the linear balance equation to initialize the wind field was examined. In all cases, the forecasts remained meteorological and reasonably well-behaved. The forecasts using winds analytically derived were virtually free of small scale inertial-gravity motions, while the forecasts using winds from the linear balance equation excited intertial-gravity waves which were large and undesirable for operational forecasts.

Therefore, an important question to be answered is what method of balancing should be used to initialize the global model so that it will not suffer during the early part of the forecast run from excitation of excessive inertial gravity motions. A number of solutions have been proposed by Myakoda and Moyer (1968), Nitta and Hovermale (1969), and Winninghoff (1971).

The method examined by Winninghoff used the equations in the model itself in an iterative sense either at a fixed time level or even in a four dimensional sense in which data is assimilated into a running model. This allows for

the natural adjustment mechanism itself to achieve the desired balance. A time scheme such as the Euler-backward may be used for selective damping of high frequency waves. The iterative method proposed by Winninghoff has the advantage of mathematical simplicity and complete consistency with the prediction model. Unfortunately, Winninghoff (1971) estimates that the iterative procedure must continue for an equivalent of an 18 to 24 hour forecast. This, of course, is not operationally feasible at the present time.

Consequently, the technique which is now being tested by FNWC utilizes the best vertical mass structure possible obtained by the latest variational analysis techniques available and then solves the complete balance equation at each level in order to get the initial wind fields. This initialization along with other helpful operationally tested devices such as smoothing, turning friction on slowly and not calling on convective adjustment for the first several time steps should be a satisfactory interim solution to this most difficult problem.

LIST OF REFERENCES

1. Arakawa, Akio, Katayama, Akira, and Mintz, "Numerical Simulation of the General Circulation of the Atmosphere," Proceedings of the WMO/IUGG Symposium on Numerical Weather Prediction, Tokyo, Japan, November 26 - December 4, 1968, Japan Meteorological Agency, Tokyo, Mar. 1969, pp. IV-1 - IV-14.

2. Arakawa, Akio, "Computational Design for Long-Term Numerical Integration of the Equations of Fluid Motion: Two Dimensional Incompressible Flow. Part I," Journal of Computational Physics, Vol. 1, No. 1, Academic Press, Inc., New York, N.Y., Jan. 1966, pp. 119-143.

3. Burington and Torrance, Higher Mathematics, p. 424-429, McGraw-Hill, 1939.

4. Dickson, Robert R., and Posey, Julian, "Maps of Snow-Cover Probability for the Northern Hemisphere," Monthly Weather Review, Vol. 95, No. 6, June 1965, p. 347-353.

5. Gates, W. L., "On the Truncation Error, Stability and Convergence of Difference Solutions of the Barotropic Vorticity Equation," J. Meteor., V. 16, p. 556-568, 1959.

6. Gates, W. L., and Riegel, C. A., "A Study of Numerical Errors in the Integration of Barotropic Flow on a Spherical Grid," J. of Geoph. Res., V. 67, No. 2, p. 773-784, Feb. 1962.

7. Haltiner, G. J., Numerical Weather Prediction, p. 1-39, 90-114, 193-196 and 220-243, Wiley, 1971.

8. Haltiner, G. J., and Martin, F. L., Dynamical and Physical Meteorology, p. 52-53, McGraw-Hill, 1957.

9. Haurwitz, B., 1940: The Motion of Atmospheric Disturbances. J. Marine Research (Sears Foundation), V. 3, p. 35-50.

10. Haurwitz, B., 1940: The Motion of Atmospheric Disturbances on the Spherical Earth. J. Marine Research (Sears Foundation), V. 3, p. 254-267.

11. Heburn, G. W., Numerical Experiments with Several Time Differencing Schemes with a Barotropic Primitive Equation Model on a Spherical Grid, M. S. Thesis, Naval Postgraduate School, 1972.

12. Jeffreys and Jeffreys, Methods of Mathematical Physics, p. 429-431, Cambridge, 1956.

13. Kesel and Winninghoff, "The Fleet Numerical Weather Central Operational Primitive-Equation Model," Mon. Wea. Rev., V. 100, No. 5, p. 360-373, 1972.

14. Kreyszig, E., Advanced Engineering Mathematics, p. 175-178, Wiley, 1962.

15. Moyer, R. W. and Miyokoda, K., "A Method of Initialization for Dynamical Weather Prediction," Tellus, V. 20, p. 115-128, 1968.

16. Naval Postgraduate School Report NPS-51Wu71081A, Restorative-Iterative Initialization for a Global Prediction Model, by F. J. Winninghoff, September 1971.

17. Neamtan, S. M., "The Motion of Harmonic Waves in the Atmosphere," J. Meteorology, V. 3, p. 53-56, 1946.

18. Nitta, T. and Hovermale, J. B., "A Technique of Objective Analysis and Initialization for the Primitive Forecast Equations," Mon. Wea. Rev., V. 97, p. 652-658, 1969.

19. Philips, N. A., "The General Circulation of the Atmosphere: a Numerical Experiment," Quart. J. Meteor. Soc., V. 82, p. 123-164, 1956.

20. Rossby, C. G. et al., "Relations Between Variations in the Intensity of the Zonal Circulation of the Atmosphere and the Displacements of the Semi-Permanent Centers of Action," J. Marine Res. (Sears Foundation), V. 2, p. 38-55, 1939.

21. UCLA Department of Meteorology Technical Report No. 3, Description of the Mintz-Arakawa Numerical General Circulation Model, by W. E. Langlois and C. W. Kwok, 1969.

22. Smagorinsky et al., "Numerical Results From a Nine-Level General Circulation Model of the Atmosphere," Monthly Weather Review, Vol. 93, No. 12, Dec. 1965, pp. 727-768.

INITIAL DISTRIBUTION LIST

		No. Copies
1.	Defense Documentation Center Cameron Station Alexandria, Virginia 22314	2
2.	Library, Code 0212 Naval Postgraduate School Monterey, California 93940	2
3.	Dr. George J. Haltiner Chairman, Department of Meteorology Naval Postgraduate School Monterey, California 93940	5
4.	Associate Professor Roger T. Williams Code 51 Department of Meteorology Naval Postgraduate School Monterey, California 93940	5
5.	Lieutenant William T. Elias Fleet Numerical Weather Central Naval Postgraduate School Monterey, California 93940	5
6.	Officer in Charge Environmental Prediction Research Facility Naval Postgraduate School Monterey, California 93940	1
7.	Commanding Officer Fleet Numerical Weather Central Naval Postgraduate School Monterey, California 93940	1
8.	LCDR Wayne R. Lambertson Fleet Numerical Weather Central Naval Postgraduate School Monterey, California 93940	1
9.	ARCRL - Research Library L. G. Hanscom Field Attn: Nancy Davis/Stop 29 Bedford, Massachusetts 01730	1
10.	Director, Naval Research Laboratory Attn: Tech. Services Info. Officer Washington, D. C. 20390	1

11. American Meteorological Society — 1
45 Beacon Street
Boston, Massachusetts 02128

12. Department of Meteorology — 3
Code 51
Naval Postgraduate School
Monterey, California 93940

13. Department of Oceanography — 1
Code 58
Naval Postgraduate School
Monterey, California 93940

14. Office of Naval Research — 1
Department of the Navy
Washington, D. C. 20360

15. Commander, Air Weather Service — 2
Military Airlift Command
U.S. Air Force
Scott Air Force Base, Illinois 62226

16. Atmospheric Sciences Library — 1
National Oceanographic Atmospheric
Administration
Silver Spring, Maryland 20910

17. National Center for Atmospheric Research — 1
Box 1470
Boulder, Colorado 80302

18. Dr. T. N. Krishnamurti — 1
Department of Meteorology
Florida State University
Tallahassee, Florida 32306

19. Dr. Fred Shuman — 1
Director
National Meteorological Center
Environmental Science Services
Administration
Suitland, Maryland 20390

20. Dr. J. Smagorinsky — 1
Director
Geophysical Fluid Dynamics Laboratory
Princeton University
Princeton, New Jersey 08540

21. Dr. A. Arakawa — 1
Department of Meteorology
UCLA
Los Angeles, California 90024

22. Professor N. A. Phillips 1
54-1422
M. I. T.
Cambridge, Massachusetts 02139

23. Dr. Russell Elsberry 1
Department of Meteorology
Naval Postgraduate School
Monterey, California 93940

24. Dr. Jerry D. Mahlman 1
Geophysical Fluid Dynamics Laboratory
Princeton University
Princeton, New Jersey 08540

25. Dr. Robert L. Haney 1
Department of Meteorology
Naval Postgraduate School
Monterey, California 93940

26. Dr. Ron L. Albertv 1
National Severe Storm Laboratory
1616 Halley Circle
Norman, Oklahoma

27. Dr. W. L. Gates 1
The RAND Corporation
1700 Main Street
Santa Monica, California 90406

28. Dr. Richard Alexander 1
The Rand Corporation
1700 Main Street
Santa Monica, California 90406

29. Commanding Officer 1
Fleet Weather Central
Box 110
FPO San Francisco 96610

30. Dr. F. J. Winninghoff 1
Department of Meteorology
UCLA
Los Angeles, California 90024

31. LCDR P. G. Kesel 1
ODSI
2460 Garden Road
Monterey, California 93940

32. Mr. Leo C. Clarke 1
FNWC
Naval Postgraduate School
Monterey, California 93940

33. Naval Weather Service Command 1
Washington Navy Yard
Washington, D. C. 20390

Security Classification

DOCUMENT CONTROL DATA - R & D

(Security classification of title, body of abstract and indexing annotation must be entered when the overall report is classified)

ORIGINATING ACTIVITY (Corporate author)

Naval Postgraduate School
Monterey, California 93940

2a. REPORT SECURITY CLASSIFICATION

Unclassified

2b. GROUP

REPORT TITLE

Numerical Experiments with a Five-Level Global Atmospheric Prediction Model Using a Staggered, Spherical, Sigma Coordinate System

DESCRIPTIVE NOTES (Type of report and inclusive dates)

Master's Thesis; March 1973

AUTHOR(S) (First name, middle initial, last name)

William Theodore Elias

REPORT DATE	7a. TOTAL NO. OF PAGES	7b. NO. OF REFS
March 1973	65	21

CONTRACT OR GRANT NO.

PROJECT NO.

9a. ORIGINATOR'S REPORT NUMBER(S)

9b. OTHER REPORT NO(S) (Any other numbers that may be assigned this report)

DISTRIBUTION STATEMENT

Approved for public release; distribution unlimited.

SUPPLEMENTARY NOTES

12. SPONSORING MILITARY ACTIVITY

Naval Postgraduate School
Monterey, California 93940

ABSTRACT

Three cases of analytic data and one case of real data wer numerically integrated using a 5-level baroclinic primitive equations model of the general circulation. Experiments were performed using initial winds derived from the linear balance equation and also winds derived analytically. The feasibility of using the linear balance equation to initialize the wind field was examined. In all cases, the forecasts remained meteorological and reasonably well-behaved. Nevertheless, the forecasts derived from initial winds generated by the linear balance equation excited large, operationally-undesirable inertial-gravity waves, while the forecasts from analytically determined initial winds remained free of such small scale "noise".

DD FORM 1 NOV 68 1473 (PAGE 1)

N 0101-807-6811

Security Classification

A-31408

14 KEY WORDS	LINK A		LINK B		LINK C	
	ROLE	WT	ROLE	WT	ROLE	WT
Numerical						
Atmospheric						
Global						
Baroclinic						
Staggered Grid						
Spherical Coordinates						
Sigma Coordinate System						
Primitive Equation						

Thesis
E316
c.1

142023

Elias

Numerical experiments with a five-level global atmospheric prediction model using a staggered, spherical, sigma coordinate system.